

Accepted Manuscript

Synthesis and evaluation of chalcone analogues containing a 4-oxoquinazolin-2-yl group as potential anti-tumor agents

Xue Han, Bin Peng, Bei-Bei Xiao, Sheng-Li Cao, Chao-Rui Yang, Wen-Zhu Wang, Fu-Cheng Wang, Hong-Yun Li, Xiao-Li Yuan, Ruifeng Shi, Ji Liao, Hailong Wang, Jing Li, Xingzhi Xu

PII: S0223-5234(18)30993-0

DOI: <https://doi.org/10.1016/j.ejmech.2018.11.034>

Reference: EJMECH 10891

To appear in: *European Journal of Medicinal Chemistry*

Received Date: 29 September 2018

Revised Date: 11 November 2018

Accepted Date: 14 November 2018

Please cite this article as: X. Han, B. Peng, B.-B. Xiao, S.-L. Cao, C.-R. Yang, W.-Z. Wang, F.-C. Wang, H.-Y. Li, X.-L. Yuan, R. Shi, J. Liao, H. Wang, J. Li, X. Xu, Synthesis and evaluation of chalcone analogues containing a 4-oxoquinazolin-2-yl group as potential anti-tumor agents, *European Journal of Medicinal Chemistry* (2018), doi: <https://doi.org/10.1016/j.ejmech.2018.11.034>.

This is a PDF file of an unedited manuscript that has been accepted for publication. As a service to our customers we are providing this early version of the manuscript. The manuscript will undergo copyediting, typesetting, and review of the resulting proof before it is published in its final form. Please note that during the production process errors may be discovered which could affect the content, and all legal disclaimers that apply to the journal pertain.



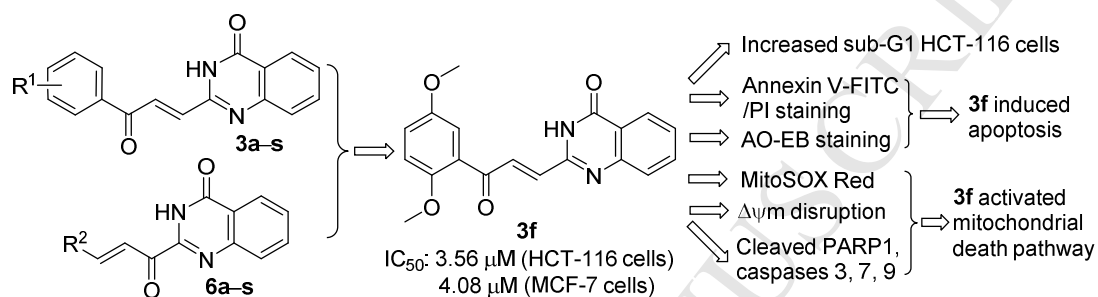
Synthesis and evaluation of chalcone analogues containing a 4-oxoquinazolin-2-yl group as potential anti-tumor agents

Xue Han^{a,1}, Bin Peng^{b,1}, Bei-Bei Xiao^{a,1}, Sheng-Li Cao^{a,*}, Chao-Rui Yang^a, Wen-Zhu Wang^a, Fu-Cheng Wang^a, Hong-Yun Li^a,
Xiao-Li Yuan^a, Ruifeng Shi^b, Ji Liao^c, Hailong Wang^c, Jing Li^c, Xingzhi Xu^{b,**}

^aDepartment of Chemistry and Beijing Key Laboratory of DNA Damage Response, Capital Normal University, Beijing 100048, PR China

^bShenzhen University School of Medicine and Guangdong Key Laboratory for Genome Stability & Disease Prevention, Shenzhen, Guangdong 518060, PR China

^cCollege of Life Science and Beijing Key Laboratory of DNA Damage Response, Capital Normal University, Beijing 100048, PR China



Synthesis and evaluation of chalcone analogues containing a 4-oxoquinazolin-2-yl group as potential anti-tumor agents

Xue Han^{a,1}, Bin Peng^{b,1}, Bei-Bei Xiao^{a,1}, Sheng-Li Cao^{a,*}, Chao-Rui Yang^a, Wen-Zhu Wang^a, Fu-Cheng Wang^a, Hong-Yun Li^a, Xiao-Li Yuan^a, Ruifeng Shi^b, Ji Liao^c, Hailong Wang^c, Jing Li^c, Xingzhi Xu^{b,**}

^aDepartment of Chemistry and Beijing Key Laboratory of DNA Damage Response, Capital Normal University, Beijing 100048, PR China

^bShenzhen University School of Medicine and Guangdong Key Laboratory for Genome Stability & Disease Prevention, Shenzhen, Guangdong 518060, PR China

^cCollege of Life Science and Beijing Key Laboratory of DNA Damage Response, Capital Normal University, Beijing 100048, PR China

Abbreviations: AO–EB, acridine orange–ethidium bromide; DAPI, 4',6-diamidino-2-phenylindole; DMSO, dimethyl sulphoxide; 5-FU, 5-Fluorouracil; FITC, fluorescein isothiocyanate; JC-1, 5,5',6,6'-tetrachloro-1,1',3,3'-tetraethylbenzimidazolcarbocyanine iodide; MTS, 3-(4,5-dimethylthiazol-2-yl)-5-(3-carboxymethoxyphenyl)-2-(4-sulfofenyl)-2H-tetrazolium, inner salt; RNS, reactive nitrogen species; ROS, reactive oxygen species; PARP1, poly(ADP-ribose) polymerase 1; PI, propidium iodide; PS, phosphatidylserine; STS, staurosporine; $\Delta\psi_m$, mitochondrial transmembrane potential.

* Corresponding author.

** Corresponding author

E-mail address: slcao@cnu.edu.cn (S.-L. Cao); xingzhi.xu@szu.edu.cn (X. Xu).

¹ These authors contributed equally to this work.

ABSTRACT:

The chalcone motif can be found in many molecules that contribute to essential biological processes, and many chalcone-containing compounds exhibit potent anti-cancer activity. Here, we synthesized two series of chalcone analogues (**3a–s** and **6a–s**) based on substituting the chalcone B-ring or A-ring with a 4-oxoquinazolin-2-yl group, and then evaluated them for cytotoxic activity in human colorectal HCT-116 and breast cancer MCF-7 cell lines. Compounds **3a–s** (in which a 4-oxoquinazolin-2-yl group functioned as the B-ring) were markedly more cytotoxic than compounds **6a–s** (in which 4-oxoquinazolin-2-yl group functioned as the A-ring), based on their IC₅₀ values to inhibit proliferation. Compound **3f** was found as the most potent among 38 analogues and the mechanism of its cytotoxicity was investigated. Flow cytometry indicated that HCT-116 cells treated with compound **3f** resulted in a dose-dependent accumulation of cells in the sub-G1 phase, which is representative of apoptotic cells. Subsequent assays (including Annexin V-FITC/PI, AO-EB, MitoSOX™ Red and JC-1 staining) confirmed that **3f** exposure induced apoptosis in HCT-116 cells. Immunoblotting analysis indicated that cellular exposure to **3f** increased the cleavage of PARP1 and caspases 3, 7, and 9. Taken together, this novel chalcone analogue has a cytotoxic effect on cultured cancer cell-lines that is likely mediated by inducing apoptosis *via* the mitochondrial death pathway.

Keywords: Quinazolin-4(3H)-one; chalcone analogue; cytotoxicity; apoptosis; mitochondrial death pathway

1. Introduction

Chalcones (1,3-diaryl-2-propen-1-ones) are natural aromatic ketones predominantly found in plants and are essential precursors for flavonoid and isoflavonoid biosynthesis. Chalcones consist of two aromatic rings (A and B rings) joined *via* a three-carbon (C) α,β -unsaturated carbonyl system (Fig. 1); the A-ring lies adjacent to the carbonyl group and the B-ring lies adjacent to the C=C double bond [1-3]. Chalcones and their synthetic analogues have attracted much attention due to their anti-cancer, anti-malarial, anti-microbial, anti-viral, and anti-inflammatory activities [3,4], and have guided the design and discovery of many anti-cancer agents [5-7].

Recent attempts to develop anti-cancer chalcone analogues have been based on the addition of various substituents to the A-ring and/or B-ring, or the replacement of these rings with heteroaryl

groups [3-9]. Introducing an imidazolone group onto the A-ring produced a chalcone analogue (Fig. 1, **I**; R = 3,4,5-triOCH₃, R¹ = Phenyl) with anti-proliferative activity towards cultured MCF-7, HT-29 and HCT-116 cancer-cell lines (IC₅₀ = 0.31, 0.66 and 0.33 μM, respectively) [8]. Exposure of MCF-7 cells to a high concentration (10 μM) of this compound arrested the cell cycle in G2/M phase. Replacing the B-ring with an indole ring also generated a chalcone analogue with potent anti-proliferative activity against cultured cancer cell lines (Fig. 1, **II**; IC₅₀ = 3–9 nM) [9]. Further investigation revealed that this compound inhibited tubulin polymerization to arrest the cell cycle at G2/M phase, thus inducing apoptosis together with a decrease in mitochondrial membrane potential.

Quinazoline is an important heterocycle, and compounds derived from its C5 or C6 position have been the main source of antifolates used in cancer chemotherapy [10,11]. Raltitrexed, a 2-methylquinazolin-4(3*H*)-one analogue of folate, has been available in a number of countries for the first-line treatment of colorectal cancer [12]. AG337 is a 2-aminoquinazolin-4(3*H*)-one derivative bearing a lipophilic side chain at the C5 position, which had entered phase II/III trial in patients with advanced hepatocellular carcinoma [13]. Derived from the C6 position of 2,4-diaminoquinazoline, trimetrexate have been reached clinical trials for treatment of solid tumors such as colorectal cancer, gastric cancer and osteosarcoma [14,15]. Many quinazolin-4(3*H*)-ones with substituents at the C2-position also exhibit anti-cancer activity [16,17]. Ispinesib is a quinazoline-based drug that inhibits the kinesin spindle protein and prevents spindle assembly and mitosis. This inhibitor reached phase II clinical trials in patients with metastatic hepatocellular carcinoma, but despite being well-tolerated, no conclusive benefit to ispinesib monotherapy was reported [18,19]. Another study synthesized 30 derivatives of 2-phenylquinazolin-4(3*H*)-one and upon testing for cytotoxic activity in human cancer cell lines found that one (Fig. 1, **III**) could induce G0/G1 phase arrest in HeLa cells [17]. Recently, we incorporated dithiocarbamate into the 2-position of quinazolin-4(3*H*)-one and found that one of the derivatives (Fig. 1, **IVc**) inhibited HT29 cell proliferation and arrested the cell cycle at G2/M phase [20]. Cellular exposure to this compound promoted tubulin polymerization and subsequent activation of the spindle assembly checkpoint [20].

Apoptosis is a cell death process accompanied by the activation of caspase proteases [21]. The mitochondrial (the intrinsic) pathway and the death receptor (DR) (the extrinsic) pathway are two major mechanisms triggering apoptotic cell death. DR-induced apoptosis requires an interaction

between a classical ligand (e.g., tumor necrosis factor (TNF)) and its cell surface receptor (e.g., TNF receptor (TNFR)) and is essential for immune system function and homeostasis. On the other hand, both excessive environmental stress (e.g., induction by genotoxic agents) and endogenous cellular stress (e.g., induction by reactive oxygen species (ROS) and unfolded proteins) actively engage apoptosis. The mitochondrial death pathway to apoptosis is a major channel of physiological cell death and a promising therapeutic target for human diseases [22]. Chalcone analogues exert cytotoxic activity through different molecular mechanisms, of which apoptosis induction is a major mechanism underlying cytotoxicity in various cancer-cell lines [5-7]. Notably, quinazoline has been recognized as a privileged structure for the development of anti-cancer agents [23]. In the present study, we therefore substituted either the A-ring or B-ring of chalcone with a 4-oxoquinazolin-2-yl group to generate a new set of chalcone analogues **3a-s** and **6a-s** (Schemes 1 and 2), and evaluated their cytotoxic activity in cultured human cancer-cell lines.

< Figure 1 >

2. Results and discussion

2.1. Synthesis

Scheme 1 outlines the synthetic pathway to derive chalcone analogues (**3a-s**) in which the B-ring was substituted with a 4-oxoquinazolin-2-yl group. In step 1, reacting methyl 2-aminobenzoate with triethyl orthoacetate and ammonium acetate under reflux for 30 h gave 2-methylquinazolin-4(3*H*)-one (intermediate **1**). In step 2, this product was oxidized with selenium dioxide to yield the 2-formyl-quinazolin-4(3*H*)-one (intermediate **2**), as previously described [24]. It is interesting that use of 1,4-dioxane as a solvent instead of ethanol (as reported in the literature [24]) shortened the reaction time from 12–15 h to 2 h, and attenuated the demethylation side reaction that otherwise occurs under prolonged periods of heating. Finally, condensation of this intermediate with various acetophenones under alkaline conditions generated 19 chalcone analogues (compounds **3a-s**) with quinazolin-4(3*H*)-one as the B-ring.

< Scheme 1 >

Scheme 2 outlines the synthetic pathway to derive chalcone analogues (**6a-s**) in which the A-ring was substituted with quinazolin-4(3*H*)-one. In step 1, reaction of methyl 2-aminobenzoate with triethyl orthopropionate and ammonium acetate generated 2-ethylquinazolin-4(3*H*)-one (intermediate **4**). In

step 2, this product was oxidized by selenium dioxide to generate the 2-acetylquinazolin-4(3*H*)-one (intermediate **5**). Finally, condensation of intermediate **5** with different aromatic aldehydes or heteroaromatic aldehydes, under alkaline conditions yielded 19 chalcone analogues (**6a–s**) with quinazolin-4(3*H*)-one as the A-ring.

< Scheme 2 >

The final reactions producing compounds **3a–s** and **6a–s** were monitored by thin-layer chromatograph (TLC) or high performance liquid chromatography (HPLC); only one spot or peak corresponding to the product was observed. Moreover, ¹H NMR spectral analysis of **3a–s** and **6a–s** indicated that each proton on carbon atoms of the C=C double bond existed as a single doublet, with a coupling constant of 15.6 or 16.2 Hz. All synthetic compounds (**3a–s** and **6a–s**) contained a C=C double bond in the three-carbon chain that can exist as a *Z*-isomer and/or *E*-isomer. The chemical analyses of **3a–s** and **6a–s**, however, suggest that they exist as geometrical *E*-isomers.

2.2. Cytotoxic activity

The cytotoxic activity of compounds **3a–s** and **6a–s** towards human colorectal HCT-116 and breast cancer MCF-7 cells was evaluated by MTS cell proliferation assay. Inhibition of cell proliferation was determined 72 h after exposure to 20 μM of each compound. The compounds that induced ≥50% inhibition compared to vehicle were considered “active”. The effects of these active compounds were further analyzed across a range of concentrations to determine the IC₅₀ values for 50% inhibition of cellular proliferation (Tables 1, 2 and 3). 5-Fluorouracil (5-FU) was used as a positive control.

Compounds **3a–s** have a 4-oxoquinazolin-2-yl group to serve as a B-ring, and a phenyl or substituted phenyl group as an A-ring. Sixteen (**3a–h**, **3j–q**) of nineteen final compounds exhibited a cytotoxic effect on cultured HCT-116 and MCF-7 cells (IC₅₀ < 20 μM); seven compounds (**3b**, **3e**, **3f**, **3j**, **3l**, **3n** and **3o**) were the most potent (IC₅₀ < 5 μM). Among seven active compounds six contained electron-donating group(s) (methoxy, hydroxyl and methyl groups) on the benzene ring, and only one compound (**3o**) had a weak electron-withdrawing group (R¹ = 4'-Br) on the benzene ring. Furthermore, compounds with a strong electron-withdrawing group, namely, **3r** (R¹ = 4'-F) or **3s** (R¹ = 4'-CF₃), were inactive (IC₅₀ > 20 μM). These results suggest that electron-donating groups at the benzene ring in chalcone analogues are more favourable for cytotoxic activity than electron-withdrawing groups. When

comparing the cytotoxic activity of closely related compounds in HCT-116 and MCF-7 cells, we found that **3b** ($R^1 = 2\text{-OCH}_3$) was more potent than **3c** ($R^1 = 3\text{-OCH}_3$) and **3d** ($R^1 = 4\text{-OCH}_3$); **3e** ($R^1 = 2,4\text{-diOCH}_3$), **3f** ($R^1 = 2,5\text{-diOCH}_3$) and **3g** ($R^1 = 2,4,6\text{-triOCH}_3$) were more potent than **3h** ($R^1 = 3,4,5\text{-triOCH}_3$). These results imply that the presence of a methoxy group at the 2-position of the benzene ring is critical for cytotoxic activity. As an example, compound **3f** ($R^1 = 2,5\text{-diOCH}_3$) had relatively low IC_{50} values of 3.56 and 4.08 μM in HCT-116 and MCF-7 cells, respectively. In pyrazolic chalcone analogues synthesized by Hawash *et al.* [25], three 2,5-dimethoxyphenyl-containing analogues were very active against cancer cells tested (Huh-7, MCF-7 and HCT-116), which is similar to our results in this study.

< Table 1 >

We also synthesized chalcone analogues **6a–s**, in which the 4-oxoquinazolin-2-yl group serves as the A-ring, and a benzene ring or a heterocycle serves as the B-ring. Only six of the nineteen compounds with a quinazolin-4(3*H*)-one ring as the A-ring (**6c**, **6g**, and **6k–n**) exhibited weak cytotoxicity in HCT-116 cells, and two of these (**6c**, **6g**) also exhibited weak cytotoxicity in MCF-7 cells (IC_{50} , 13.20–19.77 μM). All these active compounds contained a substituted benzene ring as the B-ring. Compounds containing a heterocycle (such as thiophene, furan or pyridine) as the B-ring were inactive in the cancer-cell lines tested. The active compounds were more active in HCT-116 than MCF-7 cells, as determined by MTS assay, but were all less potent than the **3a–s** series in terms of their IC_{50} . It had been disclosed in a review article that heteroaryl moieties either as the A-ring or B-ring appear to enhance the cytotoxic activity of chalcones against many types of cancer cells [6]. Nevertheless, our results clearly indicate that the 4-oxoquinazolin-2-yl group as a B-ring substitute is critical for cytotoxic activity.

< Table 2 >

Furthermore, the cytotoxicity of selective potent compounds **3b**, **3e**, **3f**, **3j**, **3l**, **3n** and **3o** ($IC_{50} < 5 \mu\text{M}$ in both HCT-116 and MCF-7 cells) were tested in other human cancer cells including A549 (lung cancer), HeLa (cervical carcinoma), HT-29 (colorectal cancer) and MD-MBA-231 (triple-negative breast cancer) as well as normal cells, MCF-10A (human breast epithelial cells) (Table 3). These compounds exhibited obvious cytotoxicity in the tested cancer cells with IC_{50} values ranging from 6.18 to 19.49 μM , with the exception of compound **3o** in HT29 cells ($IC_{50} > 20 \mu\text{M}$). All these compounds

were cytotoxic to MCF-10A cells, while the IC_{50} of **3f** for MCF-10A (9.81 μ M) is more than doubled of that for MCF-7. As in HCT-116 and MCF-7 cells, compound **3f** ($R^1 = 2',5'$ -diCH₃O) also had relatively low IC_{50} values in A549, HeLa, HT29 and MD-MBA-231 cells. Quinazoline derivatives modified at C6 position (e.g., raltitrexed, trimetrexate) are major chemotherapeutic agents for colorectal cancer [12,15], while there are no quinazoline derivatives modified at C2 position in clinical use. Furthermore, **3f** exhibited decent cytotoxicity against the triple-negative breast cancer, which lacks target therapy options [26]. Thus, it was taken forward for further investigation into the mechanisms underlying cytotoxicity in cancer cells.

< Table 3 >

2.3. Cell cycle profiling of HCT-116 cells following compound **3f** exposure

MTS assay indicated that compound **3f** had the most cytotoxic effect on HCT-116 cells compared to all other chalcone analogues ($IC_{50} = 3.56 \mu$ M). We next used flow cytometry to analyze the effects of HCT-116 cell exposure to compound **3f** on the cell-cycle profile (Fig. 2). We treated HCT-116 cells with various concentrations of compound **3f** (0.5 \times , 1.0 \times and 2.0 \times IC_{50}), 5-FU (IC_{50}), or Taxol (0.2 μ M) for 24 h and then analyzed cellular DNA content (Fig. 2A, B). 5-FU is an inhibitor of thymidylate synthase (TS), which blocks DNA synthesis and arrests the cell cycle in S phase. Taxol promotes microtubule assembly and protects the microtubule polymer from disassembly, thus arresting the cell cycle in G2/M phase. We observed a significant, dose-dependent increase in the proportion of sub-G1 HCT-116 cells in response to **3f** exposure, and no marked effect on the composition of other cell-cycle phases (Fig. 2). Based on these data, **3f** may elicit the fragmentation or degradation of nuclear DNA to form hypodiploid cells with < 2N DNA content, and induce cell apoptosis.

< Figure 2 >

2.4. Detection of apoptosis induced by **3f** by Annexin V-FITC/PI dual staining assay

We next performed an Annexin V-FITC/propidium iodide (PI) dual staining assay to confirm whether compound **3f** can induce apoptosis. Phosphatidylserine (PS) locates on the cytosolic (inner) side of the cell membrane, and translocates to the extracellular (outer) surface during early apoptosis. Annexin V has a high affinity for PS, and thus when fluorescently labelled with fluorescein isothiocyanate (FITC), can be used to identify early-stage apoptotic cells. Propidium iodide (PI) is a fluorescent intercalating agent that cannot cross the membrane of live cells. The membranes of cells in

the latter stages of apoptosis and dead cells are permeable to PI, and their nuclei stain red. We exposed HCT-116 cells or MCF-10A cells to **3f** ($1\times$ or $2\times$ IC_{50}) for 24 h or staurosporine (STS; $1\ \mu\text{M}$) for 12 h, and then stained the cells with Annexin V-FITC and PI (Fig. 3). STS is an ATP-competitive kinase inhibitor that induces apoptosis [27,28] and was used as a positive control. Annexin V-FITC-positive HCT-116 cells or MCF-10A cells were detected following both **3f** and STS treatment, in a dose-dependent manner (Fig. 3). We found that the percentage of Annexin V-FITC-positive cells induced by **3f** at the dose of $2\times$ IC_{50} in HCT-116 cells was equivalent to that induced by STS (Fig. 3A and 3B), whereas the percentage of apoptotic cells induced by the same dose of **3f** in MCF-10A cells was only 54% of that induced by STS (Fig. 3C and 3D). These data demonstrate that **3f** induces apoptosis in both colorectal cancer cells HCT-116 and immortalized mammary epithelial cells MCF-10A, indicating that **3f** has a higher potency inducing apoptosis in cancer cells than immortalized normal cells.

< Figure 3 >

2.5. Detection of apoptosis in HCT-116 cells induced by compound 3f, using AO-EB double staining assay

We performed an additional assay, based on acridine orange-ethidium bromide (AO-EB) double staining to confirm that **3f** induces apoptosis in HCT-116 cells. AO is a nucleic acid fluorescent cationic dye that stains live and dead cells green, and EB stains cells with lost membrane integrity orange [29]. HCT-116 cells were treated with compound **3f** ($1\times$ or $2\times$ IC_{50}) for 24 h or STS for 12 h, stained with AO-EB and then visualized by fluorescence microscopy (Fig. 4). Few cells treated with DMSO alone (negative control) underwent apoptosis, whereas the majority of cells treated with STS (positive control) became apoptotic. Cells treated with **3f** also underwent apoptosis, and the percentage of orange fluorescent-stained cells increased dose-dependently. These data support that **3f** induces apoptosis in HCT-116 cells.

< Figure 4 >

2.6. Mitochondrial involvement in 3f-induced apoptosis of HCT-116 cells, determined by MitoSOX™ Red assay and mitochondrial membrane potential detection

Mitochondria stress or damage initiates apoptosis by increasing the permeability of the outer mitochondrial membrane. This effect results in the release of pro-apoptotic factors into the cytosol and

an increase in cytosolic levels of reactive oxygen species (ROS), such as superoxide anions and hydrogen peroxide and reactive nitrogen species (RNS) [30]. We investigated whether **3f**-induced apoptosis was due to increased cellular ROS levels by using the fluoroprobe MitoSOXTM Red, which selectively detects superoxide in the mitochondria of live cells. MitoSOXTM Red localizes within mitochondria, is oxidized specifically by superoxide, binds mitochondrial DNA and then emits a red fluorescence [30,31]. We treated HCT-116 cells with compound **3f** (1× or 2× IC₅₀) for 24 h, or STS (1 μM) for 12 h, and then stained with MitoSOXTM Red. We found that a red fluorescence was emitted in response to both STS and **3f** exposure, which increased with the increasing dose of **3f** (Fig. 5A).

The depolarization of mitochondrial transmembrane potential ($\Delta\psi_m$) could be induced by the opening of mitochondrial permeability transition pore when apoptosis happens [32]. The metachromatic fluorochrome JC-1 (5,5',6,6'-tetrachloro-1,1',3,3'-tetraethylbenzimidazolcarbocyanine iodide) has been widely used for the detection of mitochondrial transmembrane potential ($\Delta\psi_m$) depolarization [33]. In unperturbed condition, JC-1 is more concentrated in the mitochondrial matrix (driven there by the $\Delta\psi_m$), where it forms red-emitting aggregates. Apoptosis induced the loss of red fluorescence and the gain of green-emitting monomers in cytoplasmic due to the disruption of mitochondrial transmembrane potential ($\Delta\psi_m$) [34]. We treated HCT-116 cells with compound **3f** (2× IC₅₀) for 24 h, or STS (1 μM) for 12 h, and then stained with JC-1. The JC-1 staining demonstrated that **3f**, in line with STS treatment, resulted in red fluorescence loss while green fluorescence accumulation, indicating that they dissipated the mitochondrial transmembrane potential ($\Delta\psi_m$) (Fig. 5B). These data demonstrate that compound **3f** induces apoptosis *via* the mitochondrial death pathway, elevating mitochondrial superoxide generation and depolarizing mitochondrial transmembrane potential ($\Delta\psi_m$).

< Figure 5 >

2.7. Effects of compound **3f** on caspase cleavage in HCT-116 cells

Apoptosis is governed by a cascade of caspase protein cleavage, which amplifies apoptotic signalling [35]. Apoptotic caspases are divided into two categories: initiator caspases (2, 8, 9 and 10) and executioner caspases (caspase 3, 6 and 7). Initiator caspases are activated by dimerization, followed by auto-proteolytic cleavage. Once activated, initiator caspases cleave and activate executioner caspases, leading to degradation of cellular components for apoptosis [35,36]. Poly(ADP-ribose) polymerase 1 (PARP1) is a response factor involved in DNA repair. During the early

stages of apoptosis, PARP1 is cleaved by executioner caspases. The cleaved PARP1 (89 kDa) is a hallmark of early apoptosis [37].

We exposed HCT-116 cells to compound **3f** ($2\times IC_{50}$) for 4, 8 and 12 h and then analyzed the expression of apoptosis-related proteins by Western blotting. After 12 h incubation we observed marked accumulation of cleaved PARP1, caspase 3, caspase 7 and caspase 9 (Fig. 6). Cleaved caspase 9 was detected after only 8 h exposure, which is consistent with its initiator-caspase function. Cleavage of these proteins in response to **3f** exposure support that compound **3f** initiates and executes apoptosis, by inducing the mitochondrial death pathway.

< Figure 6 >

3. Conclusions

Using a bioisosteric replacement approach, we designed and synthesized two series of chalcone analogues, known as **3a-s** and **6a-s**, whereby a 4-oxoquinazolin-2-yl group replaced the B-ring or A-ring, respectively. Compounds within the **3a-s** series were more cytotoxic than **6a-s** in HCT-116 and MCF-7 cells, and among the **3a-s** series **3f** exhibited significant cytotoxic effect with an IC_{50} of 3.56 and 4.08 μM in HCT-116 and MCF-7 cells, respectively. Moreover, **3f** had the potential of killing triple-negative breast cancer cells, and **3f** was less cytotoxic towards normal MCF-10A cells. We thus chose compound **3f** for further analysis to determine the mechanisms underlying **3f**-induced cytotoxicity. HCT-116 cells treated with compound **3f** accumulated in the sub-G1 phase of the cell cycle, indicating that these cells underwent apoptosis. This effect occurred in a dose-dependent manner with increasing doses of compound **3f**, but little effect of **3f** was found on the overall cell cycle profile. We then confirmed that compound **3f** induced apoptosis by Annexin V-FITC/PI dual staining, AO-EB staining, MitoSOX™ Red, and JC-1 staining assays. Finally, Western blot analysis indicated that treatment of HCT-116 cells with **3f** caused an increase of cleaved PARP1 and cleaved caspases 3, 7, and 9, suggesting that this compound might induce the mitochondrial death pathway. However, its molecular mechanism how this compound targets and induces apoptosis warrant further investigation. Nevertheless, these data open avenues for the development of new anti-cancer compounds based on chalcone analogues with a 4-oxoquinazolin-2-yl group.

4. Experimental procedures

4.1. Chemistry

The melting points of all compounds were determined using XT5B microscopic melting point apparatus and are presented uncorrected. ^1H and ^{13}C NMR spectra were recorded on a Varian VNMRS-600 spectrometer at 600 MHz or 150 MHz using tetramethylsilane (TMS) as an internal standard (Abbreviations: Ph = phenyl, Quin = quinazolin-4(3H)-one). High-resolution mass spectra (electrospray ionization) (HRMS (ESI)) were recorded on a Thermo Scientific LTQ Orbitrap Discovery (Bremen, Germany) mass spectrometer. Column chromatography was carried out on a silica gel (200–300 mesh). High performance liquid chromatography (HPLC) analyses were performed on an Agilent 1200 Series HPLC instrument with a G1314B VWD (variable-wavelength detector), and the profiles are presented in the supplementary materials. The purity of target compounds used in the biological studies was in general $\geq 95\%$. All the chemical reagents were commercially available and used without further purification, unless noted.

4.1.1. Preparation of 2-methylquinazolin-4(3H)-one (intermediate 1)

A mixture of methyl 2-aminobenzoate (6.04 g, 40 mmol), ammonium acetate (7.7 g, 0.1 mol) and triethyl orthoacetate (25 mL, 0.28 mol) was heated under reflux for 30 h. The solution cooled to room temperature, and the separated solid was collected by filtration and air-dried. The crude product was purified by re-crystallization from ethanol to give intermediate **1** as a white solid (4.86 g, 76%), mp 226–229 °C (Lit. [38] mp 230–232°C). ^1H NMR (600 MHz, DMSO- d_6) δ : 2.35 (s, 3H, CH₃), 7.44 (t, J = 7.8 Hz, 1H, Quin 6-H), 7.56 (d, J = 7.8 Hz, 1H, Quin 8-H), 7.76 (td, J = 7.8, 1.2 Hz, 1H, Quin 7-H), 8.07 (dd, J = 7.8, 1.2 Hz, 1H, Quin 5-H), 12.18 (br s, 1H, NH). HRMS (ESI) m/z : calcd for C₉H₉N₂O ([M+H]⁺): 161.0715; found: 161.0708.

4.1.2. Preparation of 2-formylquinazolin-4(3H)-one (intermediate 2)

A mixture of 2-methylquinazolin-4(3H)-one (intermediate **1**) (0.48 g, 3 mmol) and selenium dioxide (0.66 g, 6 mmol) in 1,4-dioxane (50 mL) was heated under reflux for 2 h. After cooling to room temperature, the mixture was filtered to remove a small amount of precipitate, and the filtrate was adjusted with 5% aqueous sodium bicarbonate to pH 7. The separated solid was removed by filtration, and the filtrate was extracted four times with dichloromethane (15 mL, each). The combined extracts were washed with brine, and then dried over anhydrous sodium sulfate overnight. The solvent was

removed by rotary evaporation, and the residue was re-crystallized from methanol to produce intermediate **2** as a light yellow solid (0.35 g, 67%), mp 135–138°C (Lit. [24] mp 138–140°C). ¹H NMR (600 MHz, DMSO-*d*₆) δ : 7.69 (td, *J* = 7.8, 1.2 Hz, 1H, Quin 6-H), 7.89 (dd, *J* = 7.8, 1.2 Hz, 1H, Quin 8-H), 7.94 (td, *J* = 7.8, 1.2 Hz, 1H, Quin 7-H), 8.21 (dd, *J* = 7.8, 1.2 Hz, 1H, Quin 5-H), 9.58 (s, 1H, CHO), 12.66 (br s, 1H, NH). HRMS (ESI) *m/z*: calcd for C₉H₇N₂O₂ ([M+H]⁺): 175.0508; found: 175.0502.

4.1.3. General preparation procedure for compounds **3a–s**

An aqueous solution of 30% potassium hydroxide (1 mL) was added to a stirred solution of the appropriate acetophenone (1.1 mmol) in methanol (10 mL). After stirring at room temperature for 20 min, 2-formylquinazolin-4(3*H*)-one (intermediate **2**; 0.17 g, 1 mmol) was added and stirring was continued for 24 h. The solution was adjusted to pH 6–7 with 6 mol/L hydrochloric acid, and the precipitate was collected by filtration and air-dried. The crude product was purified by re-crystallization from methanol to give compounds **3a–s**.

4.1.3.1. (*E*)-2-(3-Oxo-3-phenylprop-1-enyl)quinazolin-4(3*H*)-one (**3a**)

Yield: 41%, white solid, mp 231–233 °C. HPLC retention time (rt) = 4.873 min (100%). ¹H NMR (600 MHz, DMSO-*d*₆) δ : 7.34 (d, *J* = 16.2 Hz, 1H, =CHCO), 7.58 (t, *J* = 7.8 Hz, 1H, Quin 6-H), 7.64 (t, *J* = 7.8 Hz, 2H, Ph 3'-H, 5'-H), 7.74 (t, *J* = 7.8 Hz, 1H, Ph 4'-H), 7.78 (d, *J* = 7.8 Hz, 1H, Quin 8-H), 7.87 (td, *J* = 7.8, 1.2 Hz, 1H, Quin 7-H), 8.15 (d, *J* = 7.8 Hz, 2H, Ph 2'-H, 6'-H), 8.17 (dd, *J* = 7.8, 1.2 Hz, 1H, Quin 5-H), 8.39 (d, *J* = 16.2 Hz, 1H, =CH), 12.65 (s, 1H, NH). ¹³C NMR (150 MHz, DMSO-*d*₆) δ : 122.19, 126.38, 128.04, 128.29, 129.17 (2C), 129.48 (2C), 130.70, 134.36, 135.16, 136.26, 137.09, 148.87, 150.35, 161.95, 189.10. HRMS (ESI) *m/z*: calcd for C₁₇H₁₃N₂O₂ ([M+H]⁺): 277.0977; found: 277.0972.

4.1.3.2. (*E*)-2-(3-(2-Methoxyphenyl)-3-oxoprop-1-enyl)quinazolin-4(3*H*)-one (**3b**)

Yield: 31%, yellow solid, mp 225–227 °C. HPLC rt = 5.370 min (97%). ¹H NMR (600 MHz, DMSO-*d*₆) δ : 3.91 (s, 1H, OCH₃), 7.10 (t, *J* = 7.8 Hz, 1H, Ph 5'-H), 7.20 (d, *J* = 15.6 Hz, 1H, =CHCO), 7.25 (d, *J* = 7.8 Hz, 1H, Ph 3'-H), 7.56 (t, *J* = 7.8 Hz, 1H, Quin 6-H), 7.58 (d, *J* = 7.8 Hz, 1H, Ph 6'-H), 7.62 (td, *J* = 7.8, 1.2 Hz, 1H, Ph 4'-H), 7.74 (d, *J* = 7.8 Hz, 1H, Quin 8-H), 7.85 (t, *J* = 7.8 Hz, 1H, Quin 7-H), 7.98 (d, *J* = 15.6 Hz, 1H, =CH), 8.14 (d, *J* = 7.8 Hz, 1H, Quin 5-H), 12.58 (s, 1H, NH). ¹³C NMR (150 MHz, DMSO-*d*₆) δ : 56.44, 112.96, 121.15, 122.14, 126.33, 127.81, 128.13, 128.22, 130.31,

134.49, 134.50, 135.06, 135.25, 148.86, 150.36, 158.65, 161.92, 191.77. HRMS (ESI) m/z : calcd for $C_{18}H_{15}N_2O_3$ ($[M+H]^+$): 307.1083; found: 307.1080.

4.1.3.3. (*E*)-2-(3-(3-Methoxyphenyl)-3-oxoprop-1-enyl)quinazolin-4(3H)-one (**3c**)

Yield: 30%, white solid, mp 236–238 °C. HPLC rt = 6.512 min (95%). 1H NMR (600 MHz, DMSO- d_6) δ : 3.87 (s, 3H, OCH₃), 7.32 (d, J = 7.8 Hz, 1H, Ph 4'-H), 7.33 (d, J = 15.6 Hz, 1H, =CHCO), 7.56 (t, J = 7.8 Hz, 1H, Quin 6-H), 7.58 (t, J = 7.8 Hz, 1H, Ph 5'-H), 7.61 (s, 1H, Ph 2'-H), 7.76 (d, J = 7.8 Hz, 1H, Quin 8-H), 7.78 (d, J = 7.8 Hz, 1H, Ph 6'-H), 7.87 (t, J = 7.8 Hz, 1H, Quin 7-H), 8.17 (d, J = 7.8 Hz, 1H, Quin 5-H), 8.36 (d, J = 15.6 Hz, 1H, =CH), 12.63 (s, 1H, NH). ^{13}C NMR (150 MHz, DMSO- d_6) δ : 55.90, 113.66, 117.78, 120.34, 121.75, 122.18, 126.38, 128.07, 128.30, 130.66, 135.15, 136.38, 138.47, 148.86, 150.35, 160.11, 161.94, 188.81. HRMS (ESI) m/z : calcd for $C_{18}H_{15}N_2O_3$ ($[M+H]^+$): 307.1083; found: 307.1076.

4.1.3.4. (*E*)-2-(3-(4-Methoxyphenyl)-3-oxoprop-1-enyl)quinazolin-4(3H)-one (**3d**)

Yield: 35%, yellow solid, mp 239–241 °C. HPLC rt = 6.361 min (96%). 1H NMR (600 MHz, DMSO- d_6) δ : 3.90 (s, 3H, OCH₃), 7.14 (d, J = 9.0 Hz, 2H, Ph 3'-H, 5'-H), 7.30 (d, J = 15.6 Hz, 1H, =CHCO), 7.58 (t, J = 7.8 Hz, 1H, Quin 6-H), 7.77 (d, J = 7.8 Hz, 1H, Quin 8-H), 7.87 (td, J = 7.8, 1.2 Hz, 1H, Quin 7-H), 8.15 (d, J = 9.0 Hz, 2H, Ph 2'-H, 6'-H), 8.17 (dd, J = 7.8, 1.2 Hz, 1H, Quin 5-H), 8.39 (d, J = 15.6 Hz, 1H, =CH), 12.62 (s, 1H, NH). ^{13}C NMR (150 MHz, DMSO- d_6) δ : 55.70, 114.34 (2C), 121.70, 125.92, 127.52, 127.80, 129.62, 130.36, 131.22 (2C), 134.69, 135.10, 148.45, 150.06, 161.51, 163.84, 186.64. HRMS (ESI) m/z : calcd for $C_{18}H_{15}N_2O_3$ ($[M+H]^+$): 307.1083; found: 307.1074.

4.1.3.5. (*E*)-2-(3-(2,4-Dimethoxyphenyl)-3-oxoprop-1-enyl)quinazolin-4(3H)-one (**3e**)

Yield: 18%, yellow solid, mp 185–187 °C. HPLC rt = 5.082 min (95%). 1H NMR (600 MHz, DMSO- d_6) δ : 3.88 (s, 3H, OCH₃), 3.94 (s, 3H, OCH₃), 6.69 (dd, J = 8.4, 2.4 Hz, 1H, Ph 5'-H), 6.73 (d, J = 2.4 Hz, 1H, Ph 3'-H), 7.22 (d, J = 15.6 Hz, 1H, =CHCO), 7.56 (t, J = 7.8 Hz, 1H, Quin 6-H), 7.69 (d, J = 8.4 Hz, 1H, Ph 6'-H), 7.74 (d, J = 7.8 Hz, 1H, Quin 8-H), 7.85 (td, J = 7.8, 1.2 Hz, 1H, Quin 7-H), 8.14 (d, J = 15.6 Hz, 1H, =CH), 8.14 (dd, J = 7.8, 1.2 Hz, 1H, Quin 5-H), 12.58 (s, 1H, NH). ^{13}C NMR (150 MHz, DMSO- d_6) δ : 56.16, 56.57, 99.08, 106.84, 120.82, 122.10, 126.31, 127.65, 128.19, 132.88, 133.28, 135.02, 135.82, 148.95, 150.58, 161.29, 161.98, 165.20, 188.73. HRMS (ESI) m/z : calcd for $C_{19}H_{17}N_2O_4$ ($[M+H]^+$): 337.1188; found: 337.1184.

4.1.3.6. (*E*)-2-(3-(2,5-Dimethoxyphenyl)-3-oxoprop-1-enyl)quinazolin-4(3*H*)-one (**3f**)

Yield: 41%, yellow solid, mp 185–187 °C. HPLC rt = 5.247 min (96%). ¹H NMR (600 MHz, DMSO-*d*₆) δ: 3.77 (s, 3H, OCH₃), 3.86 (s, 3H, OCH₃), 7.11 (m, 1H, Ph 6'-H), 7.19 (m, 2H, Ph 3'-H, 4'-H), 7.21 (d, *J* = 15.6 Hz, 1H, =CHCO), 7.56 (td, *J* = 7.8, 1.2 Hz, 1H, Quin 6-H), 7.74 (d, *J* = 7.8 Hz, 1H, Quin 8-H), 7.85 (td, *J* = 7.8, 1.2 Hz, 1H, Quin 7-H), 7.99 (d, *J* = 15.6 Hz, 1H, =CH), 8.14 (dd, *J* = 7.8, 1.2 Hz, 1H, Quin 5-H), 12.58 (s, 1H, NH). ¹³C NMR (150 MHz, DMSO-*d*₆) δ: 56.05, 56.94, 114.41, 114.55, 120.21, 122.15, 126.33, 127.82, 128.23, 128.48, 134.59, 135.07, 135.17, 148.86, 150.34, 152.92, 153.53, 161.91, 191.37. HRMS (ESI) *m/z*: calcd for C₁₉H₁₇N₂O₄ ([M+H]⁺): 337.1188; found: 337.1184.

4.1.3.7. (*E*)-2-(3-Oxo-3-(2,4,6-trimethoxyphenyl)prop-1-enyl)quinazolin-4(3*H*)-one (**3g**)

Yield: 50%, yellow solid, mp 212–214 °C. HPLC rt = 3.779 min (99%). ¹H NMR (600 MHz, DMSO-*d*₆) δ: 3.76 (s, 6H, 2OCH₃), 3.86 (s, 3H, OCH₃), 6.35 (s, 2H, Ph 3'-H, 5'-H), 6.99 (d, *J* = 16.2 Hz, 1H, =CHCO), 7.48 (d, *J* = 16.2 Hz, 1H, =CH), 7.55 (td, *J* = 7.8, 1.2 Hz, 1H, Quin 6-H), 7.71 (d, *J* = 7.8 Hz, 1H, Quin 8-H), 7.84 (td, *J* = 7.8, 1.2 Hz, 1H, Quin 7-H), 8.12 (dd, *J* = 7.8, 1.2 Hz, 1H, Quin 5-H), 12.49 (s, 1H, NH). ¹³C NMR (150 MHz, DMSO-*d*₆) δ: 56.02, 56.39 (2C), 91.55 (2C), 110.60, 122.09, 126.32, 127.84, 128.17, 135.06, 135.52, 136.74, 148.80, 150.33, 158.91 (2C), 161.83, 163.09, 192.80. HRMS (ESI) *m/z*: calcd for C₂₀H₁₉N₂O₅ ([M+H]⁺): 367.1294; found: 367.1292.

4.1.3.8. (*E*)-2-(3-Oxo-3-(3,4,5-trimethoxyphenyl)prop-1-enyl)quinazolin-4(3*H*)-one (**3h**)

Yield: 53%, orange solid, mp 223–225 °C. HPLC rt = 6.052 min (95%). ¹H NMR (600 MHz, DMSO-*d*₆) δ: 3.80 (s, 3H, OCH₃), 3.92 (s, 6H, 2OCH₃), 7.33 (d, *J* = 15.6 Hz, 1H, =CHCO), 7.44 (s, 2H, Ph 2'-H, 6'-H), 7.59 (td, *J* = 7.8, 1.2 Hz, 1H, Quin 6-H), 7.78 (d, *J* = 7.8 Hz, 1H, Quin 8-H), 7.88 (td, *J* = 7.8, 1.2 Hz, 1H, Quin 7-H), 8.17 (dd, *J* = 7.8, 1.2 Hz, 1H, Quin 5-H), 8.35 (d, *J* = 15.6 Hz, 1H, =CH), 12.60 (s, 1H, NH). ¹³C NMR (150 MHz, DMSO-*d*₆) δ: 56.28 (2C), 60.27, 106.53 (2C), 121.66, 125.96, 127.62, 127.73, 130.08, 131.91, 134.71, 135.79, 142.73, 148.26, 149.99, 153.01 (2C), 161.54, 187.28. HRMS (ESI) *m/z*: calcd for C₂₀H₁₉N₂O₅ ([M+H]⁺): 367.1294; found: 367.1290.

4.1.3.9. (*E*)-2-(3-(4-Aminophenyl)-3-oxoprop-1-enyl)quinazolin-4(3*H*)-one (**3i**)

Yield: 14%, orange red solid, mp 253–255 °C. HPLC rt = 2.418 min (95%). ¹H NMR (600 MHz, DMSO-*d*₆) δ: 6.37 (s, 2H, NH₂), 6.66 (d, *J* = 8.4 Hz, 2H, Ph 3'-H, 5'-H), 7.24 (d, *J* = 15.6 Hz, 1H, =CHCO), 7.57 (t, *J* = 7.8 Hz, 1H, Quin 6-H), 7.76 (d, *J* = 7.8 Hz, 1H, Quin 8-H), 7.86 (t, *J* = 7.8 Hz,

1H, Quin 7-H), 7.91 (d, $J = 8.4$ Hz, 2H, Ph 2'-H, 6'-H), 8.16 (d, $J = 7.8$ Hz, 1H, Quin 5-H), 8.36 (d, $J = 15.6$ Hz, 1H, =CH), 12.58 (s, 1H, NH). ^{13}C NMR (150 MHz, DMSO- d_6) δ : 113.32 (2C), 122.07, 124.96, 126.35, 127.76, 128.17, 131.45, 131.95 (2C), 134.00, 135.09, 149.01, 150.80, 155.08, 162.03, 185.07. HRMS (ESI) m/z : calcd for $\text{C}_{17}\text{H}_{14}\text{N}_3\text{O}_2$ ($[\text{M}+\text{H}]^+$): 292.1086; found: 292.1083.

4.1.3.10. (*E*)-2-(3-(4-Hydroxyphenyl)-3-oxoprop-1-enyl)quinazolin-4(3H)-one (**3j**)

Yield: 31%, yellow solid, mp 280–282 °C. HPLC $rt = 3.427$ min (96%). ^1H NMR (600 MHz, DMSO- d_6) δ : 6.95 (d, $J = 7.8$ Hz, 2H, Ph 3'-H, 5'-H), 7.29 (d, $J = 15.6$ Hz, 1H, =CHCO), 7.58 (t, $J = 7.2$ Hz, 1H, Quin 6-H), 7.77 (d, $J = 7.2$ Hz, 1H, Quin 8-H), 7.87 (t, $J = 7.2$ Hz, 1H, Quin 7-H), 8.06 (d, $J = 7.8$ Hz, 2H, Ph 2'-H, 6'-H), 8.16 (d, $J = 7.2$ Hz, 1H, Quin 5-H), 8.38 (d, $J = 15.6$ Hz, 1H, =CH), 10.61 (s, 1H, OH), 12.61 (s, 1H, NH). ^{13}C NMR (150 MHz, DMSO- d_6 , CDCl_3) δ : 116.09 (2C), 122.09, 126.33, 127.83, 128.15, 128.75, 130.95, 131.89 (2C), 135.04, 135.13, 148.89, 150.53, 162.03, 163.36, 186.76. HRMS (ESI) m/z : calcd for $\text{C}_{17}\text{H}_{13}\text{N}_2\text{O}_3$ ($[\text{M}+\text{H}]^+$): 293.0926; found: 293.0922.

4.1.3.11. (*E*)-2-(3-(4-Hydroxy-3-methoxyphenyl)-3-oxoprop-1-enyl)quinazolin-4(3H)-one (**3k**)

Yield: 47%, yellow solid, mp 244–246 °C. HPLC $rt = 1.257$ min (100%). ^1H NMR (600 MHz, DMSO- d_6) δ : 3.90 (s, 3H, OCH_3), 6.98 (d, $J = 8.4$ Hz, 1H, Ph 5'-H), 7.30 (d, $J = 15.6$ Hz, 1H, =CHCO), 7.57 (t, $J = 7.8$ Hz, 1H, Quin 6-H), 7.61 (d, $J = 1.8$ Hz, 1H, Ph 2'-H), 7.76 (d, $J = 7.8$, 1H, Quin 8-H), 7.79 (dd, $J = 8.4$, 1.8 Hz, 1H, Ph 6'-H), 7.86 (td, $J = 7.8$, 1.2 Hz, 1H, Quin 7-H), 8.16 (dd, $J = 7.8$, 1.2 Hz, 1H, Quin 5-H), 8.38 (d, $J = 15.6$ Hz, 1H, =CH), 10.30 (s, 1H, OH), 12.60 (s, 1H, NH). ^{13}C NMR (150 MHz, DMSO- d_6) δ : 55.72, 111.54, 115.15, 121.68, 124.40, 125.93, 127.47, 127.79, 128.65, 130.36, 134.67, 134.76, 148.05, 148.49, 150.12, 152.80, 161.55, 186.23. HRMS (ESI) m/z : calcd for $\text{C}_{18}\text{H}_{15}\text{N}_2\text{O}_4$ ($[\text{M}+\text{H}]^+$): 323.1032; found: 323.1031.

4.1.3.12. (*E*)-2-(3-(2-Methylphenyl)-3-oxoprop-1-enyl)quinazolin-4(3H)-one (**3l**)

Yield: 48%, light yellow solid, mp 198–200 °C. HPLC $rt = 7.872$ min (96%). ^1H NMR (600 MHz, DMSO- d_6) δ : 2.44 (s, 3H, CH_3), 7.16 (d, $J = 15.6$ Hz, 1H, =CHCO), 7.39 (d, $J = 7.8$ Hz, 1H, Ph 3'-H), 7.41 (t, $J = 7.8$ Hz, 1H, 5'-H), 7.52 (t, $J = 7.8$ Hz, 1H, Ph 4'-H), 7.57 (t, $J = 7.8$ Hz, 1H, Quin 6-H), 7.75 (d, $J = 7.8$ Hz, 1H, Quin 8-H), 7.78 (d, $J = 7.8$ Hz, 1H, Ph 6'-H), 7.86 (t, $J = 7.8$ Hz, 1H, Quin 7-H), 7.95 (d, $J = 15.6$ Hz, 1H, =CH), 8.15 (d, $J = 7.8$ Hz, 1H, Quin 5-H), 12.59 (s, 1H, NH). ^{13}C NMR (150 MHz, DMSO- d_6) δ : 20.77, 122.14, 126.37, 127.99, 128.25, 129.56, 132.04, 132.13, 132.22, 134.12, 135.14, 136.69, 137.64, 137.90, 148.81, 150.25, 161.88, 193.93. HRMS (ESI) m/z : calcd for

$C_{18}H_{15}N_2O_2$ ($[M+H]^+$): 291.1134; found: 291.1128.

4.1.3.13. (*E*)-2-(3-(4-Methylphenyl)-3-oxoprop-1-enyl)quinazolin-4(3*H*)-one (**3m**)

Yield: 62%, white solid, mp 246–248 °C. HPLC rt = 9.081 min (95%). 1H NMR (600 MHz, DMSO- d_6) δ : 2.43 (s, 3H, CH₃), 7.32 (d, J = 15.6 Hz, 1H, =CHCO), 7.44 (d, J = 7.8 Hz, 2H, Ph 3'-H, 5'-H), 7.58 (t, J = 7.8 Hz, 1H, Quin 6-H), 7.77 (d, J = 7.8 Hz, 1H, Quin 8-H), 7.87 (td, J = 7.8, 1.2 Hz, 1H, Quin 7-H), 8.06 (d, J = 7.8 Hz, 2H, Ph 2'-H, 6'-H), 8.16 (d, J = 7.8 Hz, 1H, Quin 5-H), 8.39 (d, J = 15.6 Hz, 1H, =CH), 12.64 (s, 1H, NH). ^{13}C NMR (150 MHz, CDCl₃, CF₃CO₂D) δ : 21.82, 119.12, 121.69, 126.60, 127.98, 129.67 (2C), 130.13 (2C), 130.40, 131.22, 132.74, 138.18, 138.40, 147.66, 152.33, 161.13, 187.55. HRMS (ESI) m/z : calcd for $C_{18}H_{15}N_2O_2$ ($[M+H]^+$): 291.1134; found: 291.1129.

4.1.3.14. (*E*)-2-(3-(2,4-Dimethylphenyl)-3-oxoprop-1-enyl)quinazolin-4(3*H*)-one (**3n**)

Yield: 45%, light yellow solid, mp 200–202 °C. HPLC rt = 18.080 min (95%). 1H NMR (600 MHz, DMSO- d_6) δ : 2.37 (s, 3H, CH₃), 2.44 (s, 3H, CH₃), 7.17 (d, J = 15.6 Hz, 1H, =CHCO), 7.20 (s, 1H, Ph 3'-H), 7.22 (d, J = 7.8 Hz, 1H, Ph 5'-H), 7.57 (td, J = 7.8, 1.2 Hz, 1H, Quin 6-H), 7.75 (d, J = 7.8 Hz, 1H, Quin 8-H), 7.76 (d, J = 7.8 Hz, 1H, Ph 6'-H), 7.86 (td, J = 7.8, 1.2 Hz, 1H, Quin 7-H), 8.01 (d, J = 15.6 Hz, 1H, =CH), 8.15 (dd, J = 7.8, 1.2 Hz, 1H, Quin 5-H), 12.59 (s, 1H, NH). ^{13}C NMR (150 MHz, DMSO- d_6) δ : 21.11, 21.43, 122.13, 126.35, 126.91, 127.92, 128.23, 130.26, 132.90, 134.00, 134.68, 135.10, 136.10, 138.60, 142.59, 148.85, 150.34, 161.90, 192.77. HRMS (ESI) m/z : calcd for $C_{19}H_{17}N_2O_2$ ($[M+H]^+$): 305.1290; found: 305.1287.

4.1.3.15. (*E*)-2-(3-(4-Bromophenyl)-3-oxoprop-1-enyl)quinazolin-4(3*H*)-one (**3o**)

Yield: 58%, white solid, mp 232–234 °C. HPLC rt = 13.329 min (96%). 1H NMR (600 MHz, DMSO- d_6) δ : 7.34 (d, J = 15.6 Hz, 1H, =CHCO), 7.59 (t, J = 7.8 Hz, 1H, Quin 6-H), 7.77 (d, J = 7.8 Hz, 1H, Quin 8-H), 7.85 (d, J = 8.4 Hz, 2H, Ph 3'-H, 5'-H), 7.87 (t, J = 7.8 Hz, 1H, Quin 7-H), 8.07 (d, J = 8.4 Hz, 2H, Ph 2'-H, 6'-H), 8.16 (d, J = 7.8 Hz, 1H, Quin 5-H), 8.34 (d, J = 15.6 Hz, 1H, =CH), 12.63 (s, 1H, NH). ^{13}C NMR (150 MHz, DMSO- d_6) δ : 122.19, 126.38, 128.09, 128.30, 128.63, 130.29, 131.11 (2C), 132.56 (2C), 135.16, 136.06, 136.58, 148.84, 150.26, 161.91, 188.21. HRMS (ESI) m/z : calcd for $C_{17}H_{12}BrN_2O_2$ ($[M+H]^+$): 355.0082, 357.0062; found: 355.0080, 357.0059.

4.1.3.16. (*E*)-2-(3-(4-Chlorophenyl)-3-oxoprop-1-enyl)quinazolin-4(3*H*)-one (**3p**)

Yield: 28%, white solid, mp 231–233 °C. HPLC rt = 11.392 min (95%). 1H NMR (600 MHz, DMSO- d_6) δ : 7.33 (d, J = 15.6 Hz, 1H, =CHCO), 7.59 (t, J = 7.8 Hz, 1H, Quin 6-H), 7.70 (d, J = 8.4

Hz, 2H, Ph 3'-H, 5'-H), 7.77 (d, $J = 7.8$ Hz, 1H, Quin 8-H), 7.87 (t, $J = 7.8$ Hz, 1H, Quin 7-H), 8.15 (d, $J = 8.4$ Hz, 2H, Ph 2'-H, 6'-H), 8.16 (d, $J = 7.8$ Hz, 1H, Quin 5-H), 8.36 (d, $J = 15.6$ Hz, 1H, =CH), 12.63 (s, 1H, NH). ^{13}C NMR (150 MHz, DMSO- d_6) δ : 122.19, 126.38, 128.09, 128.29, 129.61 (2C), 130.33, 131.04 (2C), 135.16, 135.74, 136.56, 139.35, 148.84, 150.26, 161.91, 188.00. HRMS (ESI) m/z : calcd for $\text{C}_{17}\text{H}_{12}\text{ClN}_2\text{O}_2$ ($[\text{M}+\text{H}]^+$): 311.0587, 313.0558; found: 311.0585, 313.0565.

4.1.3.17. (E)-2-(3-(3,4-Dichlorophenyl)-3-oxoprop-1-enyl)quinazolin-4(3H)-one (3q)

Yield: 35%, white solid, mp 229–231 °C. HPLC rt = 18.943 min (95%). ^1H NMR (600 MHz, DMSO- d_6) δ : 7.33 (d, $J = 15.6$ Hz, 1H, =CHCO), 7.59 (t, $J = 7.8$ Hz, 1H, Quin 6-H), 7.78 (d, $J = 7.8$ Hz, 1H, Quin 8-H), 7.87 (td, $J = 7.8, 1.2$ Hz, 1H, Quin 7-H), 7.90 (d, $J = 8.4$ Hz, 1H, Ph 5'-H), 8.08 (dd, $J = 8.4, 1.8$ Hz, 1H, Ph 6'-H), 8.16 (d, $J = 7.8$ Hz, 1H, Quin 5-H), 8.33 (d, $J = 1.8$ Hz, 1H, Ph 2'-H), 8.33 (d, $J = 15.6$ Hz, 1H, =CH), 12.61 (s, 1H, NH). ^{13}C NMR (150 MHz, DMSO- d_6) δ : 122.17, 125.21, 126.40, 127.89, 128.32, 129.12, 130.98, 131.85, 132.55, 134.96, 135.23, 137.00, 137.21, 148.79, 150.20, 161.92, 187.20. HRMS (ESI) m/z : calcd for $\text{C}_{17}\text{H}_{11}\text{Cl}_2\text{N}_2\text{O}_2$ ($[\text{M}+\text{H}]^+$): 345.0198, 347.0168; found: 345.0195, 347.0164.

4.1.3.18. (E)-2-(3-(4-Fluorophenyl)-3-oxoprop-1-enyl)quinazolin-4(3H)-one (3r)

Yield: 22%, white solid, mp 252–254 °C. HPLC rt = 5.717 min (95%). ^1H NMR (600 MHz, DMSO- d_6) δ : 7.33 (d, $J = 15.6$ Hz, 1H, =CHCO), 7.47 (d, $J = 8.4$ Hz, 2H, Ph 3'-H, 5'-H), 7.59 (t, $J = 7.8$ Hz, 1H, Quin 6-H), 7.77 (d, $J = 7.8$ Hz, 1H, Quin 8-H), 7.87 (t, $J = 7.8$ Hz, 1H, Quin 7-H), 8.16 (d, $J = 7.8$ Hz, 1H, Quin 5-H), 8.24 (dd, $J = 8.4, 5.4$ Hz, 2H, Ph 2'-H, 6'-H), 8.38 (d, $J = 15.6$ Hz, 1H, =CH), 12.63 (s, 1H, NH). ^{13}C NMR (150 MHz, DMSO- d_6) δ : 116.60 (d, $J = 21.9$ Hz, 2C), 122.17, 126.40, 128.10, 128.28, 130.56, 132.27 (d, $J = 9.75$ Hz, 2C), 133.84 (d, $J = 2.1$ Hz), 135.20, 136.33, 148.84, 150.34, 161.97, 165.90 (d, $J = 251.4$ Hz), 187.68. HRMS (ESI) m/z : calcd for $\text{C}_{17}\text{H}_{12}\text{FN}_2\text{O}_2$ ($[\text{M}+\text{H}]^+$): 295.0883; found: 295.0877.

4.1.3.19. (E)-2-(3-Oxo-3-(4-(trifluoromethyl)phenyl)prop-1-enyl)quinazolin-4(3H)-one (3s)

Yield: 41%, white solid, mp 234–236 °C. HPLC rt = 9.929 min (96%). ^1H NMR (600 MHz, DMSO- d_6) δ : 7.37 (d, $J = 15.6$ Hz, 1H, =CHCO), 7.59 (t, $J = 7.8$ Hz, 1H, Quin 6-H), 7.77 (d, $J = 7.8$ Hz, 1H, Quin 8-H), 7.87 (t, $J = 7.8$ Hz, 1H, Quin 7-H), 8.0 (d, $J = 8.4$ Hz, 2H, Ph 3'-H, 5'-H), 8.16 (d, $J = 7.8$ Hz, 1H, Quin 5-H), 8.31 (d, $J = 8.4$ Hz, 2H, Ph 2'-H, 6'-H), 8.37 (d, $J = 15.6$ Hz, 1H, =CH), 12.66 (s, 1H, NH). ^{13}C NMR (150 MHz, DMSO- d_6) δ : 122.22, 124.18 (q, $J = 271.95$ Hz), 126.40, 126.43 (q,

$J = 3.9$ Hz, 2C), 128.16, 128.32, 129.95 (2C), 130.40, 133.40 (q, $J = 31.95$ Hz), 135.20, 137.05, 140.25, 148.82, 150.18, 161.90, 188.69. HRMS (ESI) m/z : calcd for $C_{18}H_{12}F_3N_2O_2$ ($[M+H]^+$): 345.0851; found: 345.0849.

4.1.4. Preparation of 2-ethylquinazolin-4(3H)-one (intermediate 4)

A mixture of methyl 2-aminobenzoate (6.04 g, 40 mmol), ammonium acetate (7.7 g, 100 mmol) and triethyl orthopropionate (25 mL) was heated under reflux for 30 h. After cooling to room temperature, the separated solid was collected by filtration and air-dried, which was re-crystallized from ethanol to give intermediate **4** as a white solid (5.01 g, 72%), mp 228–229 °C (Lit. [39] mp 229–231 °C). 1H NMR (600 MHz, DMSO- d_6) δ : 1.25 (t, $J = 7.8$ Hz, 3H, CH_2CH_3), 2.63 (q, $J = 7.8$ Hz, 2H, CH_2CH_3), 7.46 (td, $J = 7.8, 1.2$ Hz, 1H, Quin 6-H), 7.60 (d, $J = 7.8$ Hz, 1H, Quin 8-H), 7.77 (td, $J = 7.8, 1.2$ Hz, 1H, Quin 7-H), 8.09 (dd, $J = 7.8, 1.2$ Hz, 1H, Quin 5-H), 12.16 (s, 1H, NH). HRMS (ESI) m/z : calcd for $C_{10}H_{11}N_2O$ ($[M+H]^+$): 175.0871; found: 175.0865.

4.1.5. Preparation of 2-acetylquinazolin-4(3H)-one (intermediate 5)

A mixture of 2-ethylquinazolin-4(3H)-one (intermediate **4**) (0.52 g, 3 mmol) and selenium dioxide (0.66 g, 6 mmol) in 1,4-dioxane (50 mL) was heated under reflux for 1 h. After cooling to room temperature, a small amount of black solid was removed by filtration, and the filtrate was adjusted to pH 7–8 with a 5% aqueous solution of sodium bicarbonate. The separated solid was collected by filtration, and the filtrate was extracted four times with dichloromethane (15 mL, each). The combined extracts were washed with brine and dried over anhydrous sodium sulfate overnight. The solvent was removed by rotary evaporation, and the crude product was re-crystallized from methanol to produce intermediate **5** as an orange-brown solid (0.34 g, 61%), mp 174–176 °C. 1H NMR (600 MHz, DMSO- d_6) δ : 2.64 (s, 3H, CH_3CO), 7.66 (td, $J = 7.8, 1.2$ Hz, 1H, Quin 6-H), 7.85 (dd, $J = 7.8, 1.2$ Hz, 1H, Quin 8-H), 7.91 (td, $J = 7.8, 1.2$ Hz, 1H, Quin 7-H), 8.19 (dd, $J = 7.8, 1.2$ Hz, 1H, Quin 5-H), 12.25 (s, 1H, NH). HRMS (ESI) m/z : calcd for $C_{10}H_9N_2O_2$ ($[M+H]^+$): 189.0664; found: 189.0658.

4.1.6. General preparation procedure for compounds **6a–s**

An aqueous solution of 30% potassium hydroxide (1 mL) was added to a stirred solution of 2-acetylquinazolin-4(3H)-one (**5**) (0.17 g, 1 mmol) in methanol (10 mL). After 20 min stirring at room temperature, the appropriate aromatic aldehyde or heteroaromatic aldehyde (1.1 mmol) was added and stirring was continued for 24 h. The solution was adjusted to pH 6–7 with 6 mol/L hydrochloric acid.

The precipitate was collected by filtration and air-dried, which was re-crystallized from methanol to give compounds **6a**–**s**.

4.1.6.1. (*E*)-2-(3-Phenylacryloyl)quinazolin-4(3H)-one (**6a**)

Yield: 48%, brown solid, mp 171–173 °C. HPLC rt = 10.675 min (95%). ¹H NMR (600 MHz, DMSO-*d*₆) δ: 7.52 (m, 3H, Ph 3'-H, 4'-H, 5'-H), 7.69 (m, 1H, Quin 6-H), 7.87 (m, 2H, Ph 2'-H, 6'-H), 7.94 (d, *J* = 16.2 Hz, 1H, =CHCO), 7.95 (m, 2H, Quin 7-H, 8-H), 8.12 (d, *J* = 16.2 Hz, 1H, =CH), 8.22 (d, *J* = 7.8 Hz, 1H, Quin 5-H), 12.42 (s, 1H, NH). ¹³C NMR (150 MHz, DMSO-*d*₆) δ: 120.15, 123.66, 126.61, 129.09, 129.39, 129.49 (2C), 129.62 (2C), 131.83, 134.62, 135.24, 146.07, 147.65, 148.74, 161.32, 183.64. HRMS (ESI) *m/z*: calcd for C₁₇H₁₃N₂O₂ ([M+H]⁺): 277.0977; found: 277.0977.

4.1.6.2. (*E*)-2-(3-(2-Methoxyphenyl)acryloyl)quinazolin-4(3H)-one (**6b**)

Yield: 39%, brown solid, mp 175–177 °C. HPLC rt = 13.352 min (94%). ¹H NMR (600 MHz, DMSO-*d*₆) δ: 3.95 (s, 1H, OCH₃), 7.08 (t, *J* = 7.8 Hz, 1H, Ph 5'-H), 7.17 (d, *J* = 7.8 Hz, 1H, Ph 3'-H), 7.52 (t, *J* = 7.8 Hz, 1H, Ph 4'-H), 7.68 (m, 1H, Quin 6-H), 7.85 (d, *J* = 7.8 Hz, 1H, Ph 6'-H), 7.94 (m, 2H, Quin 7-H, 8-H), 8.17 (s, 2H, CH=CH), 8.22 (d, *J* = 7.8 Hz, 1H, Quin 5-H), 12.37 (s, 1H, NH). ¹³C NMR (150 MHz, DMSO-*d*₆) δ: 56.30, 112.47, 120.12, 121.37, 122.95, 123.63, 126.60, 129.11, 129.35, 129.59, 133.59, 135.21, 140.85, 147.67, 148.77, 159.20, 161.32, 183.73. HRMS (ESI) *m/z*: calcd for C₁₈H₁₅N₂O₃ ([M+H]⁺): 307.1083; found: 307.1082.

4.1.6.3. (*E*)-2-(3-(3-Methoxyphenyl)acryloyl)quinazolin-4(3H)-one (**6c**)

Yield: 47%, brown solid, mp 169–171 °C. HPLC rt = 11.509 min (98%). ¹H NMR (600 MHz, DMSO-*d*₆) δ: 3.85 (s, 3H, OCH₃), 7.10 (dd, *J* = 7.8, 1.2 Hz, 1H, Ph 4'-H), 7.41 (t, *J* = 2.4 Hz, Ph 2'-H), 7.44 (d, *J* = 7.8 Hz, 1H, Ph 6'-H), 7.45 (d, *J* = 7.8 Hz, 1H, 5'-H), 7.69 (td, *J* = 7.8, 1.2 Hz, 1H, Quin 6-H), 7.91 (d, *J* = 16.2 Hz, 1H, =CHCO), 7.94 (d, *J* = 7.8 Hz, 1H, Quin 8-H), 7.95 (d, *J* = 7.8 Hz, 1H, Quin 7-H), 8.10 (d, *J* = 16.2 Hz, 1H, =CH), 8.22 (d, *J* = 7.8 Hz, 1H, Quin 5-H), 12.42 (s, 1H, NH). ¹³C NMR (150 MHz, DMSO-*d*₆) δ: 55.72, 114.46, 117.67, 120.42, 121.70, 123.64, 126.58, 129.08, 129.33, 130.59, 135.14, 136.00, 146.03, 147.62, 148.66, 160.10, 161.28, 183.62. HRMS (ESI) *m/z*: calcd for C₁₈H₁₅N₂O₃ ([M+H]⁺): 307.1083; found: 307.1080.

4.1.6.4. (*E*)-2-(3-(4-Methoxyphenyl)acryloyl)quinazolin-4(3H)-one (**6d**)

Yield: 43%, yellow solid, mp 189–191 °C. HPLC rt = 2.030 min (100%). ¹H NMR (600 MHz, DMSO-*d*₆) δ: 3.85 (s, 3H, OCH₃), 7.07 (d, *J* = 8.4 Hz, 2H, Ph 3'-H, 5'-H), 7.68 (m, 1H, Quin 6-H), 7.84

(d, $J = 8.4$ Hz, 2H, Ph 2'-H, 6'-H), 7.91 (d, $J = 16.2$ Hz, 1H, =CHCO), 7.93 (m, 2H, Quin 7-H, 8-H), 7.98 (d, $J = 16.2$ Hz, 1H, =CH), 8.22 (d, $J = 7.8$ Hz, 1H, Quin 5-H), 12.35 (s, 1H, NH). ^{13}C NMR (150 MHz, DMSO- d_6) δ : 55.93, 115.16 (2C), 117.51, 123.60, 126.60, 127.30, 129.05, 129.27, 131.60 (2C), 135.21, 146.27, 147.72, 148.91, 161.32, 162.49, 183.40. HRMS (ESI) m/z : calcd for $\text{C}_{18}\text{H}_{15}\text{N}_2\text{O}_3$ ($[\text{M}+\text{H}]^+$): 307.1083; found: 307.1080.

4.1.6.5. (E)-2-(3-(2,4-Dimethoxyphenyl)acryloyl)quinazolin-4(3H)-one (**6e**)

Yield: 46%, yellow solid, mp 180–182 °C. HPLC rt = 12.074 min (97%). ^1H NMR (600 MHz, DMSO- d_6) δ : 3.87 (s, 3H, OCH₃), 3.95 (s, 3H, OCH₃), 6.67 (dd, $J = 8.4, 2.4$ Hz, 1H, Ph 5'-H), 6.69 (d, $J = 2.4$ Hz, 1H, Ph 3'-H), 7.67 (m, 1H, Quin 6-H), 7.81 (d, $J = 8.4$ Hz, 1H, Ph 6'-H), 7.93 (m, 2H, Quin 7-H, 8-H), 8.04 (d, $J = 16.2$ Hz, 1H, =CHCO), 8.12 (d, $J = 16.2$ Hz, 1H, =CH), 8.21 (d, $J = 7.8$ Hz, 1H, Quin 5-H), 12.28 (s, 1H, NH). ^{13}C NMR (150 MHz, DMSO- d_6) δ : 56.09, 56.42, 98.88, 107.20, 116.08, 117.19, 123.56, 126.58, 129.06, 129.20, 131.50, 135.17, 141.28, 147.74, 148.98, 161.07, 161.31, 164.29, 183.46. HRMS (ESI) m/z : calcd for $\text{C}_{19}\text{H}_{17}\text{N}_2\text{O}_4$ ($[\text{M}+\text{H}]^+$): 337.1188; found: 337.1187.

4.1.6.6. (E)-2-(3-(3,4-Dimethoxyphenyl)acryloyl)quinazolin-4(3H)-one (**6f**)

Yield 51%, yellow solid, mp 184–186 °C. HPLC rt = 3.731 min (98%). ^1H NMR (600 MHz, DMSO- d_6) δ : 3.85 (s, 3H, OCH₃), 3.88 (s, 3H, OCH₃), 7.09 (d, $J = 9.0$ Hz, 1H, Ph 5'-H), 7.46 (m, 2H, Ph 2'-H, 6'-H), 7.68 (m, 1H, Quin 6-H), 7.90 (d, $J = 16.2$ Hz, 1H, =CHCO), 7.94 (m, 2H, Quin 7-H, 8-H), 7.97 (d, $J = 16.2$ Hz, 1H, =CH), 8.21 (d, $J = 7.8$ Hz, 1H, Quin 5-H), 12.36 (s, 1H, NH). ^{13}C NMR (150 MHz, DMSO- d_6) δ : 56.13 (2C), 111.69, 112.22, 117.74, 123.58, 124.52, 126.59, 127.47, 129.06, 129.25, 135.19, 146.92, 147.72, 148.97, 149.50, 152.43, 161.32, 183.51. HRMS (ESI) m/z : calcd for $\text{C}_{19}\text{H}_{17}\text{N}_2\text{O}_4$ ($[\text{M}+\text{H}]^+$): 337.1188; found: 337.1186.

4.1.6.7. (E)-2-(3-(3,5-Dimethoxyphenyl)acryloyl)quinazolin-4(3H)-one (**6g**)

Yield: 51%, brown solid, mp 181–183 °C. HPLC rt = 12.351 min (98%). ^1H NMR (600 MHz, DMSO- d_6) δ : 3.83 (s, 6H, 2OCH₃), 6.66 (t, $J = 1.8$ Hz, 1H, Ph 4'-H), 7.02 (d, $J = 1.8$ Hz, 2H, Ph 2'-H, 6'-H), 7.68 (td, $J = 7.8, 1.2$ Hz, 1H, Quin 6-H), 7.86 (d, $J = 16.2$ Hz, 1H, =CHCO), 7.93 (td, $J = 7.8, 1.2$ Hz, 1H, Quin 7-H), 7.96 (d, $J = 7.8$ Hz, 1H, Quin 8-H), 8.07 (d, $J = 16.2$ Hz, 1H, =CH), 8.22 (d, $J = 7.8$ Hz, 1H, Quin 5-H), 12.42 (s, 1H, NH). ^{13}C NMR (150 MHz, DMSO- d_6) δ : 55.93 (2C), 103.96, 107.28 (2C), 120.86, 123.65, 126.59, 129.15, 129.38, 135.20, 136.57, 146.23, 147.64, 148.75, 161.26 (2C), 161.32, 183.82. HRMS (ESI) m/z : calcd for $\text{C}_{19}\text{H}_{17}\text{N}_2\text{O}_4$ ($[\text{M}+\text{H}]^+$): 337.1188; found: 337.1186.

4.1.6.8. (*E*)-2-(3-(3,4,5-Trimethoxyphenyl)acryloyl)quinazolin-4(3*H*)-one (**6h**)

Yield: 33%, yellow solid, mp 189–191 °C. HPLC rt = 9.931 min (96%). ¹H NMR (600 MHz, DMSO-*d*₆) δ: 3.74 (s, 3H, OCH₃), 3.89 (s, 6H, 2OCH₃), 7.21 (s, 2H, Ph 2'-H, 6'-H), 7.68 (t, *J* = 7.8 Hz, 1H, Quin 6-H), 7.89 (d, *J* = 15.6 Hz, 1H, =CHCO), 7.95 (m, 2H, Quin 7-H, 8-H), 8.01 (d, *J* = 15.6 Hz, 1H, =CH), 8.22 (d, *J* = 7.8, 1H, Quin 5-H), 12.39 (s, 1H, NH). ¹³C NMR (150 MHz, DMSO-*d*₆) δ: 56.59 (2C), 60.64, 107.23 (2C), 119.57, 123.61, 126.60, 129.10, 129.31, 130.16, 135.19, 140.92, 146.85, 147.67, 148.91, 153.62 (2C), 161.31, 183.79. HRMS (ESI) *m/z*: calcd for C₂₀H₁₉N₂O₅ ([M+H]⁺): 367.1294; found: 367.1291.

4.1.6.9. (*E*)-2-(3-(4-Methylphenyl)acryloyl)quinazolin-4(3*H*)-one (**6i**)

Yield: 39%, orange solid, mp 186–188 °C. HPLC rt = 17.735 min (96%). ¹H NMR (600 MHz, DMSO-*d*₆) δ: 2.38 (s, 3H, CH₃), 7.33 (d, *J* = 7.8 Hz, 2H, Ph 3'-H, 5'-H), 7.68 (m, 1H, Quin 6-H), 7.76 (d, *J* = 7.8 Hz, 2H, Ph 2'-H, 6'-H), 7.91 (d, *J* = 15.6 Hz, 1H, =CHCO), 7.94 (m, 2H, Quin 7-H, 8-H), 8.07 (d, *J* = 15.6 Hz, 1H, =CH), 8.22 (d, *J* = 7.8, 1H, Quin 5-H), 12.39 (s, 1H, NH). ¹³C NMR (150 MHz, DMSO-*d*₆) δ: 21.61, 118.95, 123.60, 126.60, 129.07, 129.36, 129.56 (2C), 130.25 (2C), 131.89, 135.24, 142.18, 146.20, 147.64, 148.74, 161.35, 183.52. HRMS (ESI) *m/z*: calcd for C₁₈H₁₅N₂O₂ ([M+H]⁺): 291.1134; found: 291.1132.

4.1.6.10. (*E*)-2-(3-(4-Bromophenyl)acryloyl)quinazolin-4(3*H*)-one (**6j**)

Yield: 68%, light yellow solid, mp 202–204 °C. HPLC rt = 1.704 min (95%). ¹H NMR (600 MHz, DMSO-*d*₆) δ: 7.69 (m, 1H, Quin 6-H), 7.71 (d, *J* = 8.4 Hz, 2H, Ph 3'-H, 5'-H), 7.83 (d, *J* = 8.4 Hz, 2H, Ph 2'-H, 6'-H), 7.91 (d, *J* = 16.2 Hz, 1H, =CHCO), 7.94 (m, 2H, Quin 7-H, 8-H), 8.12 (d, *J* = 16.2 Hz, 1H, =CH), 8.22 (d, *J* = 7.8, 1H, Quin 5-H), 12.43 (s, 1H, NH). ¹³C NMR (150 MHz, DMSO-*d*₆) δ: 120.90, 123.67, 125.25, 126.62, 129.09, 129.44, 131.36 (2C), 132.61 (2C), 133.90, 135.26, 144.67, 147.63, 148.69, 161.32, 183.61. HRMS (ESI) *m/z*: calcd for C₁₇H₁₂BrN₂O₂ ([M+H]⁺): 335.0082, 357.0062; found: 355.0076, 357.0060.

4.1.6.11. (*E*)-2-(3-(4-Chlorophenyl)acryloyl)quinazolin-4(3*H*)-one (**6k**)

Yield: 46%, light yellow solid, mp 198–200 °C. HPLC rt = 2.539 min (98%). ¹H NMR (600 MHz, DMSO-*d*₆) δ: 7.57 (d, *J* = 8.4 Hz, 2H, Ph 3'-H, 5'-H), 7.69 (m, 1H, Quin 6-H), 7.91 (d, *J* = 8.4 Hz, 2H, Ph 2'-H, 6'-H), 7.92 (m, 3H, Quin 7-H, 8-H; =CHCO), 8.11 (d, *J* = 16.2 Hz, 1H, =CH), 8.22 (d, *J* = 7.8, 1H, Quin 5-H), 12.43 (s, 1H, NH). ¹³C NMR (150 MHz, DMSO-*d*₆) δ: 120.87, 123.68, 126.63, 129.09,

129.43, 129.67 (2C), 131.19 (2C), 133.59, 135.25, 136.29, 144.56, 147.63, 148.69, 161.31, 183.60.

HRMS (ESI) m/z : calcd for $C_{17}H_{12}ClN_2O_2$ ($[M+H]^+$): 311.0587, 313.0558; found: 311.0587, 313.0569.

4.1.6.12. (*E*)-2-(3-(4-Fluorophenyl)acryloyl)quinazolin-4(3*H*)-one (**6l**)

Yield: 31%, pink solid, mp 189–191 °C. HPLC rt = 13.651 min (98%). 1H NMR (600 MHz, DMSO- d_6) δ : 7.35 (t, J = 8.4 Hz, 2H, Ph 3'-H, 5'-H), 7.68 (m, 1H, Quin 6-H), 7.94 (d, J = 16.2 Hz, 1H, =CHCO), 7.95 (m, 5H, Ph 2'-H, 6'-H; Quin 7-H, 8-H; =CHCO), 8.06 (d, J = 16.2 Hz, 1H, =CH), 8.22 (d, J = 7.8 Hz, 1H, Quin 5-H), 12.42 (s, 1H, NH). ^{13}C NMR (150 MHz, DMSO- d_6) δ : 116.68 (d, J = 21.75 Hz, 2C), 120.0, 123.64, 126.61, 129.06, 129.39, 131.31 (d, J = 3.0 Hz), 131.96 (d, J = 8.7 Hz, 2C), 135.23, 144.85, 147.63, 148.69, 161.32, 163.42 (d, J = 248.85 Hz), 183.57. HRMS (ESI) m/z : calcd for $C_{17}H_{12}FN_2O_2$ ($[M+H]^+$): 295.0883; found: 295.0882.

4.1.6.13. (*E*)-2-(3-(4-Cyanophenyl)acryloyl)quinazolin-4(3*H*)-one (**6m**)

Yield: 61%, pink solid, mp 200–202 °C. HPLC rt = 1.288 min (100%). 1H NMR (600 MHz, DMSO- d_6) δ : 7.69 (m, 1H, Quin 6-H), 7.95 (m, 5H, Quin 7-H, 8-H; Ph 2'-H, 6'-H; =CHCO), 8.06 (d, J = 7.8 Hz, 2H, Ph 3'-H, 5'-H), 8.21 (m, 2H, =CH, Quin 5-H), 12.48 (s, 1H, NH). ^{13}C NMR (150 MHz, DMSO- d_6 , CF_3COOD) δ : 113.31, 121.14, 121.63, 127.11, 128.83, 129.15, 129.61 (2C), 130.73, 133.05 (2C), 136.51, 138.85, 145.51, 145.95, 147.49, 163.88, 182.46. HRMS (ESI) m/z : calcd for $C_{18}H_{12}N_3O_2$ ($[M+H]^+$): 302.0930; found: 302.0926.

4.1.6.14. (*E*)-2-(3-(4-Nitrophenyl)acryloyl)quinazolin-4(3*H*)-one (**6n**)

Yield: 69%, light yellow solid, mp 206–208 °C. HPLC rt = 1.353 min (99%). 1H NMR (600 MHz, DMSO- d_6) δ : 7.70 (m, 1H, Quin 6-H), 7.95 (m, 2H, Quin 7-H, 8-H), 8.01 (d, J = 16.2 Hz, 1H, =CHCO), 8.15 (d, J = 8.4 Hz, 2H, Ph 2'-H, 6'-H), 8.23 (d, J = 8.4, 1H, Quin 5-H), 8.25 (d, J = 16.2 Hz, 1H, =CH), 8.32 (d, J = 8.4 Hz, 2H, Ph 3'-H, 5'-H), 12.50 (s, 1H, NH). ^{13}C NMR (150 MHz, DMSO- d_6) δ : 123.72, 124.09, 124.60 (2C), 126.66, 129.12, 129.56, 130.48 (2C), 135.30, 140.93, 142.94, 147.57, 148.58, 148.89, 161.32, 183.59. HRMS (ESI) m/z : calcd for $C_{17}H_{12}N_3O_4$ ($[M+H]^+$): 322.0828; found: 322.0826.

4.1.6.15. (*E*)-2-(3-(Furan-2-yl)acryloyl)quinazolin-4(3*H*)-one (**6o**)

Yield: 65%, yellow solid, mp 187–189 °C. HPLC rt = 5.546 min (97%). 1H NMR (600 MHz, DMSO- d_6) δ : 6.75 (dd, J = 3.6, 1.8 Hz, 1H, Furan-2-yl 4'-H), 7.20 (d, J = 3.6 Hz, 1H, Furan-2-yl 3'-H), 7.68 (td, J = 7.8, 1.8 Hz, 1H, Quin 6-H), 7.73 (d, J = 15.6 Hz, 1H, =CHCO), 7.87 (d, J = 15.6 Hz, 1H, =CH), 7.93 (m, 2H, Quin 7-H, 8-H), 8.01 (d, J = 1.2 Hz, 1H, Furan-2-yl 5'-H), 8.21 (d, J = 7.8, 1H,

Quin 5-H), 12.36 (s, 1H, NH). ^{13}C NMR (150 MHz, DMSO- d_6) δ : 109.98, 113.95, 116.72, 119.63, 123.62, 126.58, 129.09, 129.34, 131.89, 135.20, 147.66, 148.63, 151.41, 161.27, 183.01. HRMS (ESI) m/z : calcd for $\text{C}_{15}\text{H}_{11}\text{N}_2\text{O}_3$ ($[\text{M}+\text{H}]^+$): 267.0770; found: 267.0764.

4.1.6.16. (*E*)-2-(3-(Thiophen-2-yl)acryloyl)quinazolin-4(3H)-one (**6p**)

Yield: 37%, brown solid, mp 174–176 °C. HPLC rt = 11.772 min (94%). ^1H NMR (600 MHz, DMSO- d_6) δ : 7.25 (td, J = 4.8, 1.2 Hz, 1H, Thiophen-2-yl 4'-H), 7.67 (td, J = 7.2, 1.8 Hz, 1H, Quin 6-H), 7.76 (d, J = 4.8 Hz, 1H, Thiophen-2-yl 3'-H), 7.80 (d, J = 15.6 Hz, 1H, =CHCO), 7.88 (d, J = 4.8 Hz, 1H, Thiophen-2-yl 5'-H), 7.93 (m, 2H, Quin 7-H, 8-H), 8.12 (d, J = 15.6 Hz, 1H, =CH), 8.21 (d, J = 8.4, 1H, Quin 5-H), 12.37 (s, 1H, NH). ^{13}C NMR (150 MHz, DMSO- d_6) δ : 118.29, 123.63, 126.60, 129.11, 129.35, 129.57, 132.08, 135.13, 135.21, 138.81, 140.03, 147.62, 148.67, 161.28, 182.97. HRMS (ESI) m/z : calcd for $\text{C}_{15}\text{H}_{11}\text{N}_2\text{O}_2\text{S}$ ($[\text{M}+\text{H}]^+$): 283.0541; found: 283.0537.

4.1.6.17. (*E*)-2-(3-(Pyridin-2-yl)acryloyl)quinazolin-4(3H)-one (**6q**)

Yield: 28%, orange solid, mp 190–192 °C. HPLC rt = 3.559 min (95%). ^1H NMR (600 MHz, DMSO- d_6) δ : 7.50 (m, 1H, Pyridin-2-yl 5'-H), 7.69 (td, J = 7.8, 1.2 Hz, 1H, Quin 6-H), 7.85 (d, J = 7.8 Hz, 1H, Pyridin-2-yl 3'-H), 7.91 (d, J = 15.6 Hz, 1H, =CHCO), 7.93–7.97 (m, 3H, Quin 7-H, 8-H; Pyridin-2-yl 4'-H), 8.22 (d, J = 7.8, 1H, Quin 5-H), 8.51 (d, J = 15.6 Hz, 1H, =CH), 8.75 (d, J = 4.8 Hz, 1H, Pyridin-2-yl 6'-H), 12.44 (s, 1H, NH). ^{13}C NMR (150 MHz, DMSO- d_6) δ : 123.34, 123.71, 125.83, 126.62, 126.83, 129.15, 129.50, 135.28, 137.88, 144.40, 147.65, 148.64, 150.75, 152.55, 161.30, 183.94. HRMS (ESI) m/z : calcd for $\text{C}_{16}\text{H}_{12}\text{N}_3\text{O}_2$ ($[\text{M}+\text{H}]^+$): 278.0930; found: 278.0925.

4.1.6.18. (*E*)-2-(3-(Pyridin-3-yl)acryloyl)quinazolin-4(3H)-one (**6r**)

Yield: 48%, brown solid, mp 197–200 °C. HPLC rt = 3.408 min (95%). ^1H NMR (600 MHz, DMSO- d_6) δ : 7.54 (t, J = 6.0 Hz, 1H, Pyridin-3-yl 5'-H), 7.69 (m, 1H, Quin 6-H), 7.96 (m, 3H, Quin 7-H, 8-H; =CHCO), 8.21 (d, J = 16.2 Hz, 1H, =CH), 8.22 (d, J = 7.8, 1H, Quin 5-H), 8.34 (d, J = 7.8 Hz, 1H, Pyridin-3-yl 6'-H), 8.67 (d, J = 4.2 Hz, 1H, Pyridin-3-yl 4'-H), 9.01 (s, 1H, Pyridin-3-yl 2'-H), 12.47 (s, 1H, NH). ^{13}C NMR (150 MHz, DMSO- d_6) δ : 122.10, 123.68, 124.62, 126.63, 129.10, 129.49, 130.52, 135.27, 135.58, 142.62, 147.60, 148.60, 151.06, 152.05, 162.75, 183.58. HRMS (ESI) m/z : calcd for $\text{C}_{16}\text{H}_{12}\text{N}_3\text{O}_2$ ($[\text{M}+\text{H}]^+$): 278.0930; found: 278.0927.

4.1.6.19. (*E*)-2-(3-(Pyridin-4-yl)acryloyl)quinazolin-4(3H)-one (**6s**)

Yield: 19%, brown solid, mp 218–220 °C. HPLC rt = 3.462 min (94%). ^1H NMR (600 MHz,

DMSO- d_6) δ : 7.70 (m, 1H, Quin 6-H), 7.81 (d, $J = 6.0$ Hz, 2H, Pyridin-4-yl 2'-H, 6'-H), 7.88 (d, $J = 16.2$ Hz, 1H, =CHCO), 7.95 (m, 2H, Quin 7-H, 8-H), 8.23 (d, $J = 7.8$, 1H, Quin 5-H), 8.28 (d, $J = 16.2$ Hz, 1H, =CH), 8.72 (d, $J = 6.0$ Hz, 2H, Pyridin-4-yl 3'-H, 5'-H), 12.51 (s, 1H, NH). ^{13}C NMR (150 MHz, DMSO- d_6) δ : 123.77, 126.05 (2C), 126.53, 128.88, 129.34, 129.54, 134.84, 138.88, 142.52 (2C), 147.36, 147.90, 151.37, 161.11, 183.17. HRMS (ESI) m/z : calcd for $\text{C}_{16}\text{H}_{12}\text{N}_3\text{O}_2$ ($[\text{M}+\text{H}]^+$): 278.0930; found: 278.0927.

4.2. Biological assays

4.2.1. Cell lines and culture conditions

HCT-116 and MCF-7 cells were cultured in Dulbecco modified Eagle medium (DMEM, Hyclone) supplemented with 10% fetal bovine serum (FBS, Hyclone) and standard antibiotics (Hyclone), at 37 °C in a humidified, 5% CO_2 incubator.

4.2.2. MTS cell proliferation assay

MTS cell proliferation assay was performed as previously described [40]. Cell viability was assessed using the CellTiter 96® AQueous One Solution Cell Proliferation Assay kit (Promega). The data were obtained from triplicate wells in three independent experiments.

4.2.3. Cell cycle profile analysis of HCT-116 cells

HCT-116 cells were treated with compound **3f** (0.5 \times , 1 \times and 2 \times IC_{50}), 5-FU (IC_{50}), or taxol (0.2 μM) for 24 h. The cells were harvested with trypsin, fixed in 75% ice-cold ethanol, and stained with propidium iodide (PI) at room temperature for 30 min. The stained cells were analyzed for DNA content using a BD Accuri C6 flow cytometer (BD Biosciences, USA). The cell cycle distribution was analyzed using FlowJo software.

4.2.4. Annexin V-FITC/PI dual staining assay

The Annexin V-FITC/PI dual staining assay was used to determine the percentage of apoptotic cells. Cells (3×10^6 /mL per well) were plated in 6-well culture plates and allowed to grow for 24 h. The cells were treated with compound **3f** (1 \times or 2 \times IC_{50}) for 24 h, and then harvested with trypsin. The harvested cells were washed twice with ice-cold PBS, and incubated in the dark at room temperature in 100 mL 1 \times binding buffer containing 1 μL Annexin V-FITC and 12.5 mL PI. After 15 min incubation, cells were analyzed for percentage undergoing apoptosis using a BD Accuri C6 flow cytometer (BD Biosciences, USA).

4.2.5. Acridine orange–ethidium bromide (AO–EB) fluorescence staining assay

HCT-116 cells (3×10^6 /mL per well) were plated in 6-well culture plates and exposed to different concentrations of compound **3f** ($1\times$ or $2\times$ IC_{50}) for 24 h or staurosporine (STS; $1 \mu\text{M}$) for 12 h. The cells were washed twice with ice-cold PBS, and then stained with 1 mL of dye mixture containing $1 \mu\text{g/mL}$ AO and $1 \mu\text{g/mL}$ EB in PBS and incubated at room temperature for 5 min in the dark. The stained cells were observed under a Nikon fluorescence microscope (TE2000-U, Nikon Inc., Japan) at $10\times$ magnification, using excitation wavelength 488 nm and emission wavelength 550 nm.

4.2.6. MitoSOX™ Red staining assay

Mitochondrial superoxide production was determined using MitoSOX™ Red mitochondrial superoxide indicator. HCT-116 cells (3×10^6 /mL per well) were plated in 6-well culture plates and allowed to grow for 24 h. Cells were treated with different concentrations of compound **3f** ($1\times$ or $2\times$ IC_{50}) for 24 h or STS ($1 \mu\text{M}$) for 12 h. After treatment, cells were washed twice with ice-cold PBS and incubated with MitoSOX™ Red mitochondrial superoxide indicator ($5 \mu\text{M}$) in PBS for 10 min at 37°C in the dark. The stained cells were observed under a Nikon fluorescence microscope (TE2000-U, Nikon Inc., Japan) at $10\times$ magnification, and an excitation wavelength of 488 nm and an emission wavelength of 550 nm.

4.2.7. Mitochondrial membrane potential monitored by JC-1 staining

HCT-116 cells were seeded in 6 well plate and treated with compound **3f** ($2\times$ IC_{50}) for 24 h, or STS ($1 \mu\text{M}$) for 12 h. They were then washed with PBS, added fresh medium (1 mL) and JC-1 (5,5',6,6'-tetrachloro-1,1',3,3'-tetraethylbenzimidazolylcarbocyanine iodide, Beyotime, C2006) molecular probe (1 mL). After 20 min incubation at 37°C , rinsed twice with PBS. Visualization of JC-1 aggregates (red fluorescence) and JC-1 monomers (green fluorescence) were done using filter (emission 488 and 550 nm, respectively) by Nikon fluorescence microscope (TE2000-U, Nikon Inc., Japan) at $40\times$ magnification, and an excitation wavelength of 488 nm and an emission wavelength of 550 nm.

4.2.8. Western blotting

Cultured HCT-116 cells were treated with compound **3f** for 4, 8, or 12 h. After treatment, cells were harvested and total proteins were extracted using sample buffer (62.5 mM Tris-HCl (pH 6.8), 2% SDS, 0.05% bromophenol blue, 20% Glycerin, 5% β -mercaptoethanol). The extracted protein samples

were separated on a 4–18% gradient SDS-polyacrylamide gel and transferred onto polyvinylidene difluoride membranes. The membranes were blocked in 0.05% PBST containing 5% skim milk for 30 min at room temperature, and incubated with primary antibody overnight at 4 °C. Antibodies against PARP1 (A301-376A) and β -actin (A5441) were purchased from Bethyl Laboratories and Sigma, respectively. Antibodies against caspase 3 (9665), caspase 7 (12827) and caspase 9 (9508), cleaved caspase 3 (9664), cleaved caspase 7 (8438) and cleaved caspase 9 (7237) were purchased from Cell Signaling Technology. After washing with PBST, the membranes were incubated with HRP-conjugated Goat Anti-Mouse IgG (115-035-116) or Donkey Anti-Rabbit (711-035-152) secondary antibodies (Jackson ImmunoResearch) at room temperature for 1 h. The immunoblots were visualized with ECL reagent and imaged using ImageQuantTM LAS 4000 software (GE Healthcare Life Sciences).

4.2.9. Statistical analysis method

Student's t-test for means, chi-squared tests, Mann-Whitney U test and Kruskal-Wallis analysis of variance by ranks were considered significant for p values < 0.05.

Acknowledgments

This work was supported by the 973 project (Project No. 2013CB911002), National Natural Science Foundation of China (Project No. 31530016 and 31761133012), the Shenzhen Science and Technology Innovation Commission (Project No. JCYJ20170412113009742) and Capacity Building for Sci-Tech Innovation–Fundamental Scientific Research Funds (Grant No. 025185305000/208). The authors would like to thank Dr. Jessica Tamanini (Shenzhen University Health Science Centre and ETediting) for proof reading the manuscript prior to submission.

References

- [1] N.J. Lawrence, R.P. Patterson, L.L. Ooi, D. Cook, S. Ducki, Effects of α -substitutions on structure and biological activity of anticancer chalcones, *Biorg. Med. Chem. Lett.* 16 (2006) 5844-5848.
- [2] Y. Ivanova, G. Momekov, O. Petrov, M. Karaivanova, V. Kalcheva, Cytotoxic Mannich bases of 6-(3-aryl-2-propenoyl)-2(3H)-benzoxazolones, *Eur. J. Med. Chem.* 42 (2007) 1382-1387.
- [3] C. Zhuang, W. Zhang, C. Sheng, W. Zhang, C. Xing, Z. Miao, Chalcone: A privileged structure in

- medicinal chemistry, *Chem. Rev.* 117 (2017) 7762-7810.
- [4] P. Singh, A. Anand, V. Kumar, Recent developments in biological activities of chalcones: a mini review, *Eur. J. Med. Chem.* 85 (2014) 758-777.
- [5] D.K. Mahapatra, S.K. Bharti, V. Asati, Anti-cancer chalcones: Structural and molecular target perspectives, *Eur. J. Med. Chem.* 98 (2015) 69-114.
- [6] C. Karthikeyan, N.S. Moorthy, S. Ramasamy, U. Vanam, E. Manivannan, D. Karunagaran, P. Trivedi, Advances in chalcones with anticancer activities, *Recent Pat. Anticancer Drug Discov.* 10 (2015) 97-115.
- [7] H. Mirzaei, S. Emami, Recent advances of cytotoxic chalconoids targeting tubulin polymerization: Synthesis and biological activity, *Eur. J. Med. Chem.* 121 (2016) 610-639.
- [8] A. Kamal, G. Ramakrishna, P. Raju, A. Viswanath, M.J. Ramaiah, G. Balakishan, M. Pal-Bhadra, Synthesis and anti-cancer activity of chalcone linked imidazolones, *Biorg. Med. Chem. Lett.* 20 (2010) 4865-4869.
- [9] J. Yan, J. Chen, S. Zhang, J. Hu, L. Huang, X. Li, Synthesis, evaluation, and mechanism study of novel indole-chalcone derivatives exerting effective antitumor activity through microtubule destabilization in vitro and in vivo, *J. Med. Chem.* 59 (2016) 5264-5283.
- [10] A. Gangjee, H.D. Jain, S. Kurup, Recent advances in classical and non-classical antifolates as antitumor and antiopportunistic infection agents: part I, *Anti-cancer Agents Med. Chem.* 7 (2007) 524-542.
- [11] A. Gangjee, H.D. Jain, S. Kurup, Recent advances in classical and non-classical antifolates as antitumor and antiopportunistic infection agents: Part II, *Anti-cancer Agents Med. Chem.* 8 (2008) 205-231.
- [12] A. Avallone, E. Di Gennaro, L. Silvestro, V.R. Iaffaioli, A. Budillon, Targeting thymidylate synthase in colorectal cancer: critical re-evaluation and emerging therapeutic role of raltitrexed, *Expert Opin. Drug Saf.* 13 (2014) 113-129.
- [13] M. Jhawer, L. Rosen, J. Dancey, H. Hochster, S. Hamburg, M. Tempero, N. Clendeninn, S. Mani, Phase II trial of nolatrexed dihydrochloride [Thymitaq, AG 337] in patients with advanced hepatocellular carcinoma, *Invest. New Drugs* 25 (2007) 85-94.
- [14] C.D. Blanke, K. Chansky, K.L. Christman, S.A. Hundahl, B.F. Issell, P.J. Van Veldhuizen, Jr., G.T.

- Budd, J.L. Abbruzzese, J.S. Macdonald, S9511: a Southwest Oncology Group phase II study of trimetrexate, 5-fluorouracil, and leucovorin in unresectable or metastatic adenocarcinoma of the stomach, *Am. J. Clin. Oncol.* 33 (2010) 117-120.
- [15] C.D. Blanke, B. Kasimis, P. Schein, R. Capizzi, M. Kurman, Phase II study of trimetrexate, fluorouracil, and leucovorin for advanced colorectal cancer, *J. Clin. Oncol.* 15 (1997) 915-920.
- [16] E. Jafari, M.R. Khajouei, F. Hassanzadeh, G.H. Hakimelahi, G.A. Khodarahmi, Quinazolinone and quinazoline derivatives: recent structures with potent antimicrobial and cytotoxic activities, *Res. Pharm. Sci.* 11 (2016) 1-14.
- [17] H.K. Rhee, J.H. Yoo, E. Lee, Y.J. Kwon, H.R. Seo, Y.S. Lee, H.Y. Choo, Synthesis and cytotoxicity of 2-phenylquinazolin-4(3*H*)-one derivatives, *Eur. J. Med. Chem.* 46 (2011) 3900-3908.
- [18] J.J. Knox, S. Gill, T.W. Synold, J.J. Biagi, P. Major, R. Feld, C. Cripps, N. Wainman, E. Eisenhauer, L. Seymour, A phase II and pharmacokinetic study of SB-715992, in patients with metastatic hepatocellular carcinoma: a study of the National Cancer Institute of Canada Clinical Trials Group (NCIC CTG IND.168), *Invest. New Drugs* 26 (2008) 265-272.
- [19] L. Lad, L. Luo, J.D. Carson, K.W. Wood, J.J. Hartman, R.A. Copeland, R. Sakowicz, Mechanism of inhibition of human KSP by ispinosib, *Biochemistry* 47 (2008) 3576-3585.
- [20] P.P. Ding, M. Gao, B.B. Mao, S.L. Cao, C.H. Liu, C.R. Yang, Z.F. Li, J. Liao, H.C. Zhao, Z. Li, J. Li, H.L. Wang, X. Xu, Synthesis and biological evaluation of quinazolin-4(3*H*)-one derivatives bearing dithiocarbamate side chain at C2-position as potential antitumor agents, *Eur. J. Med. Chem.* 108 (2016) 364-373.
- [21] D.R. Green, F. Llambi, Cell Death Signaling, *Cold Spring Harb. Perspect. Biol.* 7 (2015) a006080.
- [22] S. Gupta, G.E. Kass, E. Szegezdi, B. Joseph, The mitochondrial death pathway: a promising therapeutic target in diseases, *J. Cell. Mol. Med.* 13 (2009) 1004-1033.
- [23] S. Shagufta, I. Ahmad, An insight into the therapeutic potential of quinazoline derivatives as anticancer agents, *MedChemComm* 8 (2017) 871-885.
- [24] Z.H. Khalil, A.I.M. Koraiem, M.A. El-Maghraby, R.M. Abu-El-Hamd, Synthesis, spectral behavior and biological activity of benzoxazolonyl(quinoxalonyl)benzofurano(indolo)quinoline apocyanine dyes, *J. Chem. Technol. Biotechnol.* 36 (1986) 379-388.

- [25] M.M. Hawash, D.C. Kahraman, F. Eren, R. Cetin Atalay, S.N. Baytas, Synthesis and biological evaluation of novel pyrazolic chalcone derivatives as novel hepatocellular carcinoma therapeutics, *Eur. J. Med. Chem.* 129 (2017) 12-26.
- [26] C. Neophytou, P. Boutsikos, P. Papageorgis, Molecular mechanisms and emerging therapeutic targets of triple-negative breast cancer metastasis, *Front. Oncol.* 8 (2018) 31.
- [27] H.-J. Chae, J.-S. Kang, J.-O. Byun, K.-S. Han, D.-U. Kim, S.-M. Oh, H.-M. Kim, S.-W. Chae, H.-R. Kim, Molecular mechanism of staurosporine-induced apoptosis in osteoblasts, *Pharmacol. Res.* 42 (2000) 373-381.
- [28] G. Feng, N. Kaplowitz, Mechanism of staurosporine-induced apoptosis in murine hepatocytes, *Am. J. Physiol. Gastrointest. Liver Physiol.* 282 (2002) 825-834.
- [29] K. Liu, P.C. Liu, R. Liu, X. Wu, Dual AO/EB staining to detect apoptosis in osteosarcoma cells compared with flow cytometry, *Med. Sci. Monit. Basic Res.* 21 (2015) 15-20.
- [30] P. Mukhopadhyay, M. Rajesh, G. Hasko, B.J. Hawkins, M. Madesh, P. Pacher, Simultaneous detection of apoptosis and mitochondrial superoxide production in live cells by flow cytometry and confocal microscopy, *Nat. Protoc.* 2 (2007) 2295-2301.
- [31] K.M. Robinson, M.S. Janes, M. Pehar, J.S. Monette, M.F. Ross, T.M. Hagen, M.P. Murphy, J.S. Beckman, Selective fluorescent imaging of superoxide in vivo using ethidium-based probes, *Proc. Natl. Acad. Sci. U. S. A.* 103 (2006) 15038-15043.
- [32] J.D. Ly, D.R. Grubb, A. Lawen, The mitochondrial membrane potential ($\Delta\psi_m$) in apoptosis; an update, *Apoptosis* 8 (2003) 115-128.
- [33] L. Troiano, R. Ferraresi, E. Lugli, E. Nemes, E. Roat, M. Nasi, M. Pinti, A. Cossarizza, Multiparametric analysis of cells with different mitochondrial membrane potential during apoptosis by polychromatic flow cytometry, *Nat. Protoc.* 2 (2007) 2719-2727.
- [34] E. Cavalieri, A. Rigo, M. Bonifacio, A.C.D. Prati, E. Guardalben, C. Bergamini, R. Fato, G. Pizzolo, H. Suzuki, F. Vinante, Pro-apoptotic activity of α -bisabolol in preclinical models of primary human acute leukemia cells, *J. Transl. Med.* 9 (2011) 1-13.
- [35] S.J. Riedl, Y. Shi, Molecular mechanisms of caspase regulation during apoptosis, *Nat. Rev. Mol. Cell Biol.* 5 (2004) 897-907.
- [36] S. Elmore, Apoptosis: a review of programmed cell death, *Toxicol. Pathol.* 35 (2007) 495-516.

- [37] A.H. Boulares, A.G. Yakovlev, V. Ivanova, B.A. Stoica, G. Wang, S. Iyer, M. Smulson, Role of poly(ADP-ribose) polymerase (PARP) cleavage in apoptosis. Caspase 3-resistant PARP mutant increases rates of apoptosis in transfected cells, *J. Biol. Chem.* 274 (1999) 22932-22940.
- [38] M. Okano, J. Mito, Y. Maruyama, H. Masuda, T. Niwa, S. Nakagawa, Y. Nakamura, A. Matsuura, Discovery and structure-activity relationships of 4-aminoquinazoline derivatives, a novel class of opioid receptor like-1 (ORL1) antagonists, *Biorg. Med. Chem. Lett.* 17 (2009) 119-132.
- [39] W. Xu, H. Fu, Amino acids as the nitrogen-containing motifs in copper-catalyzed domino synthesis of *N*-heterocycles, *J. Org. Chem.* 76 (2011) 3846-3852.
- [40] S.L. Cao, Y. Han, C.Z. Yuan, Y. Wang, Z.K. Xiahou, J. Liao, R.T. Gao, B.B. Mao, B.L. Zhao, Z.F. Li, X. Xu, Synthesis and antiproliferative activity of 4-substituted-piperazine-1-carbodithioate derivatives of 2,4-diaminoquinazoline, *Eur. J. Med. Chem.* 64 (2013) 401-409.

Figure captions

Fig. 1. Chemical structures of chalcones, ispinesib, synthetic chalcone analogues (**I**, **II**) and quinazoline-based compounds (**III**, **IV**).

Scheme 1. Synthetic pathway of 19 chalcone analogues (**3a–s**) with a B-ring quinazolin-4(3*H*)-one substitution. Reagents and conditions: (a) $\text{CH}_3\text{C}(\text{OC}_2\text{H}_5)_3$, AcONH_4 , reflux, 30 h. (b) SeO_2 , 1,4-dioxane, reflux, 2 h. (c) Acetophenones, CH_3OH , 30% KOH (aq.), rt, 24 h.

Scheme 2. Synthetic pathway of 19 chalcone analogues (**6a–s**) with an A-ring quinazolin-4(3*H*)-one substitution. Reagents and conditions: (a) $\text{C}_2\text{H}_5\text{C}(\text{OC}_2\text{H}_5)_3$, AcONH_4 , reflux, 30 h. (b) SeO_2 , 1,4-dioxane, reflux, 1 h. (c) R^2CHO , CH_3OH , 30% KOH (aq.), rt, 24 h.

Fig. 2. Effects of compound **3f** on cell-cycle progression in HCT-116 cells. (A) HCT-116 cells were treated with increasing concentrations of **3f** ($0.5\times$, $1\times$ or $2\times \text{IC}_{50}$), 5-FU (IC_{50}), or Taxol ($0.2 \mu\text{M}$) for 24 h before being harvested and analyzed by flow cytometry. The data represent the means \pm SD of three independent experiments. $**P < 0.001$ (Student's t-test). (B) Representative cell-cycle profiles from three independent experiments. The red arrows indicate the sub-G1 phase.

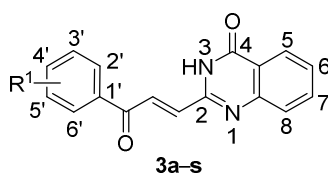
Fig. 3. Quantification of apoptotic HCT-116 cells by Annexin V-FITC/PI dual staining, following **3f** and STS treatment. (A) HCT-116 cells were treated with **3f** ($1\times$ or $2\times \text{IC}_{50}$) for 24 h or STS for 12 h. Cells were harvested and apoptotic HCT-116 cells were determined by Annexin V-FITC/PI staining and flow cytometry. Cells in the lower left quadrant (Q1-LL: Annexin V-/PI+) represent live cells; cells in the lower right quadrant (Q1-LR: Annexin V+/PI-) represent early apoptotic cells; cells in the upper right quadrant (Q1-UR: Annexin V+/PI+) represent late apoptotic cells; cells in the upper left quadrant (Q1-UL: Annexin V-/PI+) represent necrotic cells. (B) Percentage of apoptotic cells, determined as the sum of late apoptotic cells (UR) and early apoptosis cells (LR) from three separate experiments. (C) and (D) Similar analysis of apoptosis induced by **3f** and STS treatment was performed in MCF-10A cells. The data represent the means \pm SD of three independent experiments. $*P < 0.05$; $**P < 0.001$

(Student's t-test).

Fig. 4. Analysis of apoptotic HCT-116 cells by AO-EB staining, following **3f** and STS treatment. HCT-116 cells were treated with **3f** (1× or 2× IC₅₀) for 24 h or STS (1 μM) for 12 h and stained with AO-EB. Three fields-of-view were randomly selected under a fluorescence microscope, and the cells were imaged under bright field and the appropriate fluorescent channels (10× magnification).

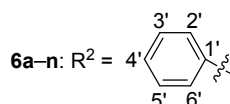
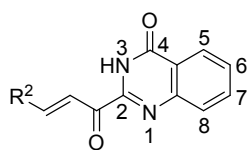
Fig. 5. Mitochondrial involvement in compound **3f**-mediated apoptosis of HCT-116 cells. (A) HCT-116 cells were treated with **3f** (1× or 2× IC₅₀) for 24 h or STS (1 μM) for 12 h and stained with MitoSOXTM Red. Two fields-of-view were randomly selected under a fluorescence microscope, and the cells were imaged under bright field, and the corresponding fluorescent channel (10× magnification). (B) The depolarization of mitochondrial transmembrane potential ($\Delta\psi_m$) could be induced by compound **3f**. HCT-116 cells were treated with compound **3f** (2× IC₅₀) for 24 h, or STS (1 μM) for 12 h, and then stained with JC-1 for 20 min at 37°C. Both the loss of red fluorescence and the gain of green-emitting monomers indicated the disruption of the mitochondrial transmembrane potential ($\Delta\psi_m$). STS served as a positive control, and the representative images were shown of the corresponding fluorescent channel (40× magnification).

Fig. 6. Effects of compound **3f** on apoptosis-related protein expression in HCT-116 cells. HCT-116 cells were treated with **3f** (2× IC₅₀) for 4, 8, and 12 h, and total lysates were harvested and immuno-blotted with various antibodies, as indicated. β -actin was used as a loading control.

Table 1. IC₅₀ values for compounds **3a–s** in cultured HCT-116 and MCF-7 cells.

Compound	R ¹	IC ₅₀ (μM) ^a	
		HCT-116	MCF-7
3a	H	5.47 ± 0.16	4.09 ± 0.17
3b	2'-OCH ₃	3.91 ± 0.06	4.30 ± 0.33
3c	3'-OCH ₃	12.00 ± 0.81	12.89 ± 0.96
3d	4'-OCH ₃	10.01 ± 0.68	10.23 ± 0.51
3e	2',4'-diOCH ₃	4.08 ± 0.04	4.49 ± 0.43
3f	2',5'-diOCH ₃	3.56 ± 0.12	4.08 ± 0.04
3g	2',4',6'-triOCH ₃	5.57 ± 0.12	5.02 ± 0.22
3h	3',4',5'-triOCH ₃	12.83 ± 2.42	13.90 ± 1.22
3i	4'-NH ₂	> 20	> 20
3j	4'-OH	4.11 ± 0.18	4.92 ± 0.06
3k	4'-OH-3'-OCH ₃	4.58 ± 0.25	6.05 ± 0.29
3l	2'-CH ₃	4.14 ± 0.05	4.20 ± 0.27
3m	4'-CH ₃	5.75 ± 0.23	9.44 ± 0.68
3n	2',4'-diCH ₃	4.77 ± 0.26	4.50 ± 0.38
3o	4'-Br	4.74 ± 0.46	3.75 ± 0.19
3p	4'-Cl	6.10 ± 0.61	6.09 ± 0.34
3q	3',4'-diCl	17.00 ± 1.98	8.21 ± 0.80
3r	4'-F	> 20	> 20
3s	4'-CF ₃	> 20	> 20
5-FU		5.53 ± 0.90	32.18 ± 1.13

^a IC₅₀: The concentration that causes 50% of cell proliferation inhibition. Data represent the means ± standard deviation from triplicate determination from three independent experiments.

Table 2. IC₅₀ values for compounds **6a–s** in cultured HCT-116 and MCF-7 cells.

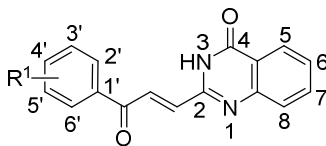
6a–n: R² = 4'-substituted benzene ring

6o–s: R² = heteroaryl groups

Compound	R ²	IC ₅₀ (μM) ^a	
		HCT-116	MCF-7
6a	C ₆ H ₅	> 20	> 20
6b	2'-OCH ₃ C ₆ H ₄	> 20	> 20
6c	3'-OCH ₃ C ₆ H ₄	14.71 ± 2.55	15.54 ± 0.91
6d	4'-OCH ₃ C ₆ H ₄	> 20	> 20
6e	2',4'-diOCH ₃ C ₆ H ₃	> 20	> 20
6f	3',4'-diOCH ₃ C ₆ H ₃	> 20	> 20
6g	3',5'-diOCH ₃ C ₆ H ₃	15.79 ± 2.05	16.76 ± 1.95
6h	3',4',5'-triOCH ₃ C ₆ H ₂	> 20	> 20
6i	4'-CH ₃ C ₆ H ₄	> 20	> 20
6j	4'-BrC ₆ H ₄	> 20	> 20
6k	4'-ClC ₆ H ₄	15.60 ± 4.32	> 20
6l	4'-FC ₆ H ₄	15.25 ± 2.08	> 20
6m	4'-CNC ₆ H ₄	19.77 ± 2.09	> 20
6n	4'-NO ₂ C ₆ H ₄	13.20 ± 1.46	> 20
6o	Furan-2-yl	> 20	> 20
6p	Thiophen-2-yl	> 20	> 20
6q	Pyridin-2-yl	> 20	> 20
6r	Pyridin-3-yl	> 20	> 20
6s	Pyridin-4-yl	> 20	> 20

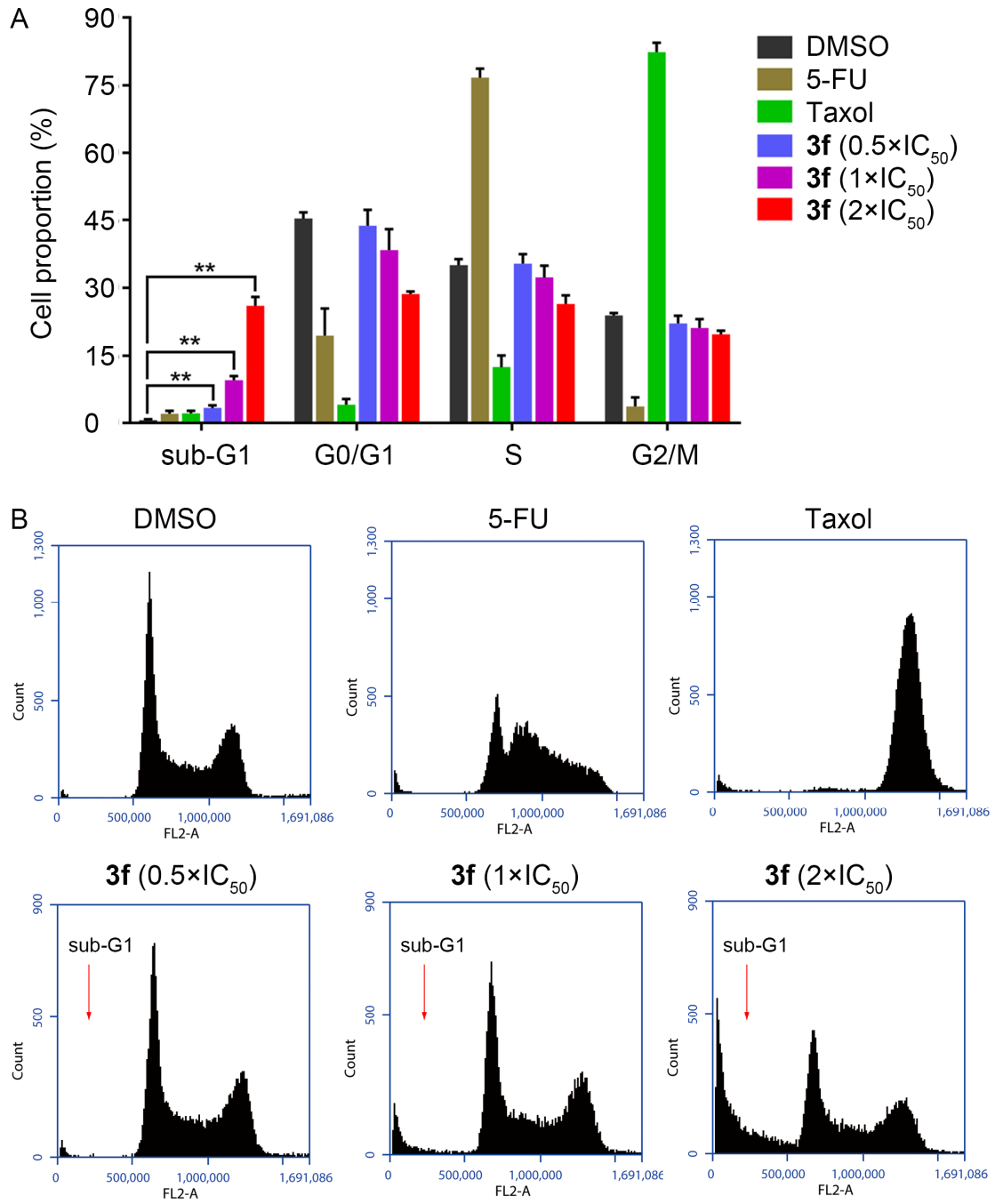
^a IC₅₀: The concentration that causes 50% of cell proliferation inhibition. Data represent the means ± standard deviation from triplicate determination from three independent experiments.

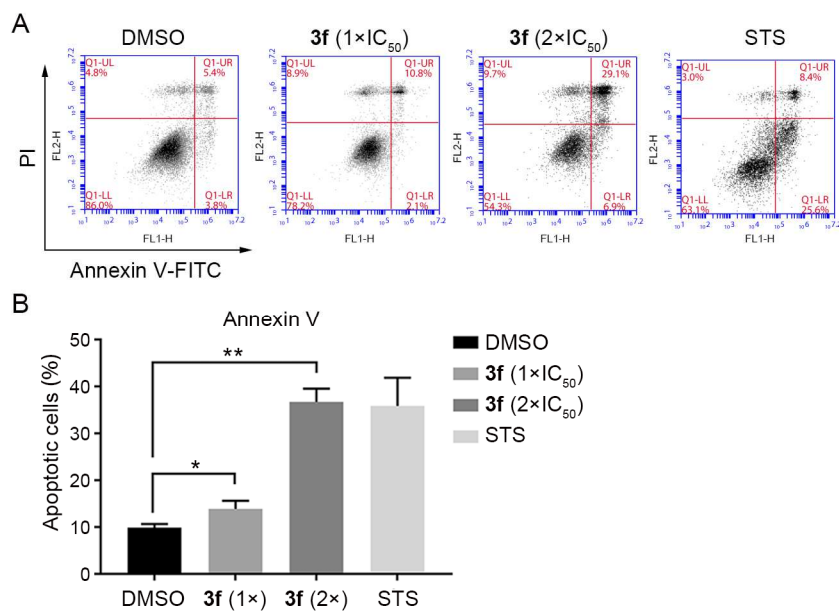
Table 3. IC₅₀ values for compounds **3b**, **3e**, **3f**, **3j**, **3l**, **3n** and **3o** in cultured A549, HeLa, HT-29, MD-MBA-231, MCF-10A and MEF cells.



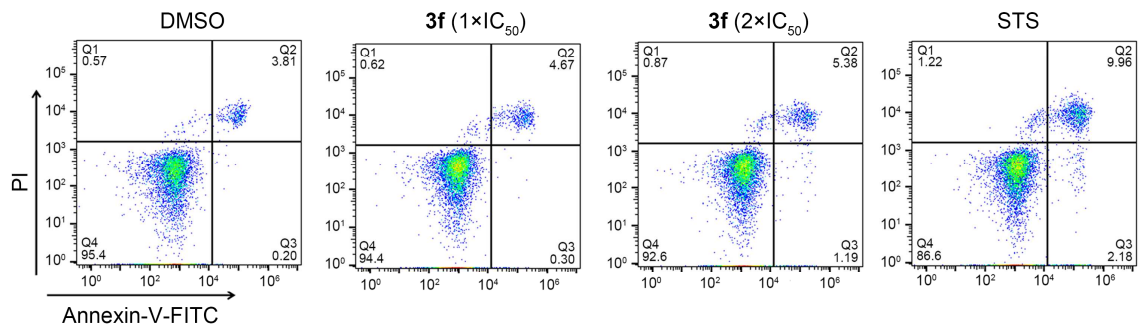
Compound	R ¹	IC ₅₀ (μM) ^a				
		A549	HeLa	HT-29	MD-MBA-231	MCF-10A
3b	2'-OCH ₃	13.68 ± 0.34	13.44 ± 0.36	6.71 ± 0.14	15.65 ± 0.32	5.26 ± 0.07
3e	2',4'-diOCH ₃	15.45 ± 0.46	12.68 ± 0.12	8.77 ± 0.26	14.34 ± 0.44	9.14 ± 0.05
3f	2',5'-diOCH ₃	12.70 ± 0.18	8.37 ± 0.26	6.18 ± 0.20	10.62 ± 0.24	9.81 ± 0.13
3j	4'-OH	15.14 ± 0.27	9.44 ± 0.41	10.65 ± 0.22	16.54 ± 0.37	6.12 ± 0.14
3l	2'-CH ₃	13.34 ± 0.37	10.40 ± 0.32	6.45 ± 0.25	10.47 ± 0.42	6.19 ± 0.11
3n	2',4'-diCH ₃	13.27 ± 0.28	9.55 ± 0.47	12.45 ± 0.35	15.29 ± 0.35	5.47 ± 0.20
3o	4'-Br	19.49 ± 0.30	16.09 ± 0.18	> 20	18.34 ± 0.46	11.34 ± 0.28
5-FU		14.96 ± 0.23	> 20	9.99 ± 0.18	> 20	> 20

^a IC₅₀: The concentration that causes 50% of cell proliferation inhibition. Data represent the means ± standard deviation from triplicate determination from three independent experiments.

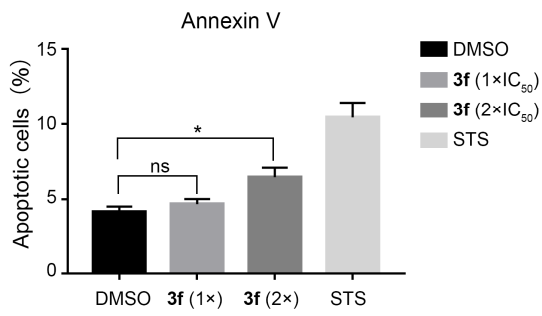


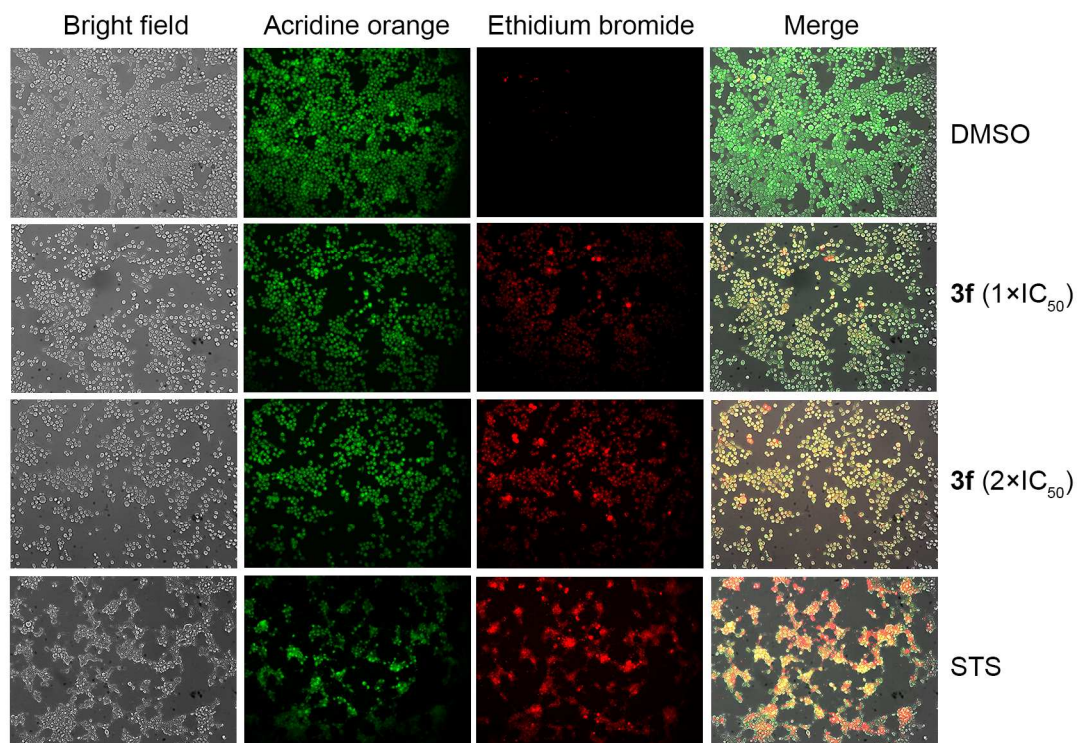


C

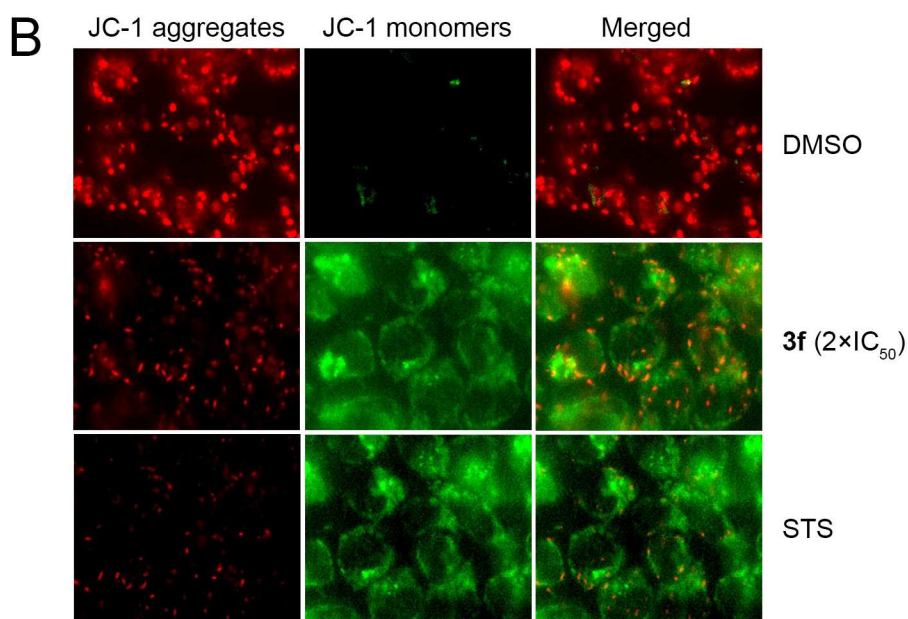
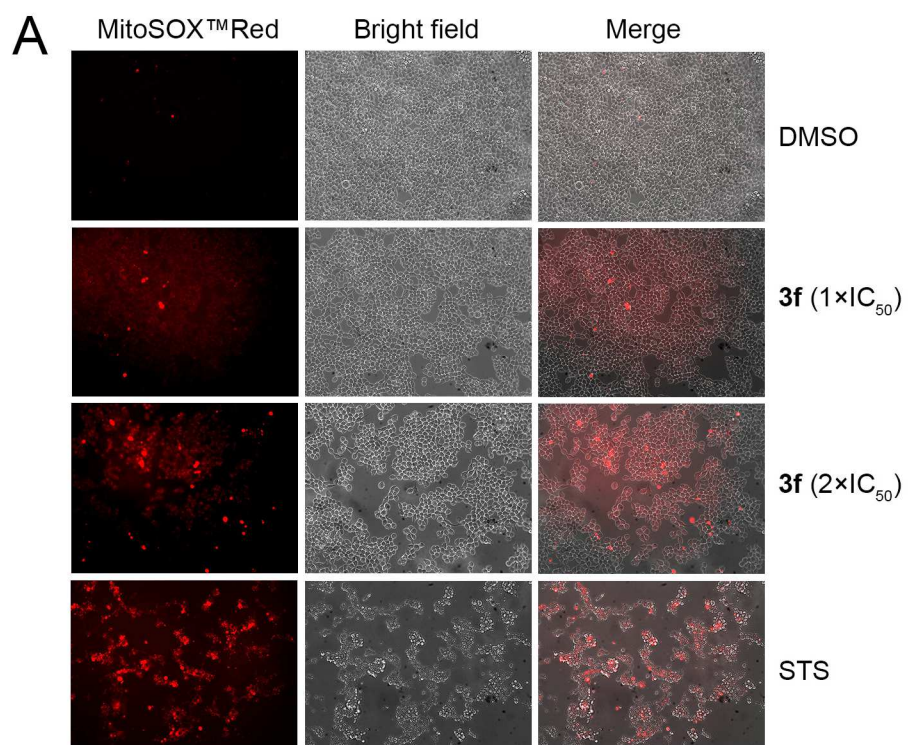


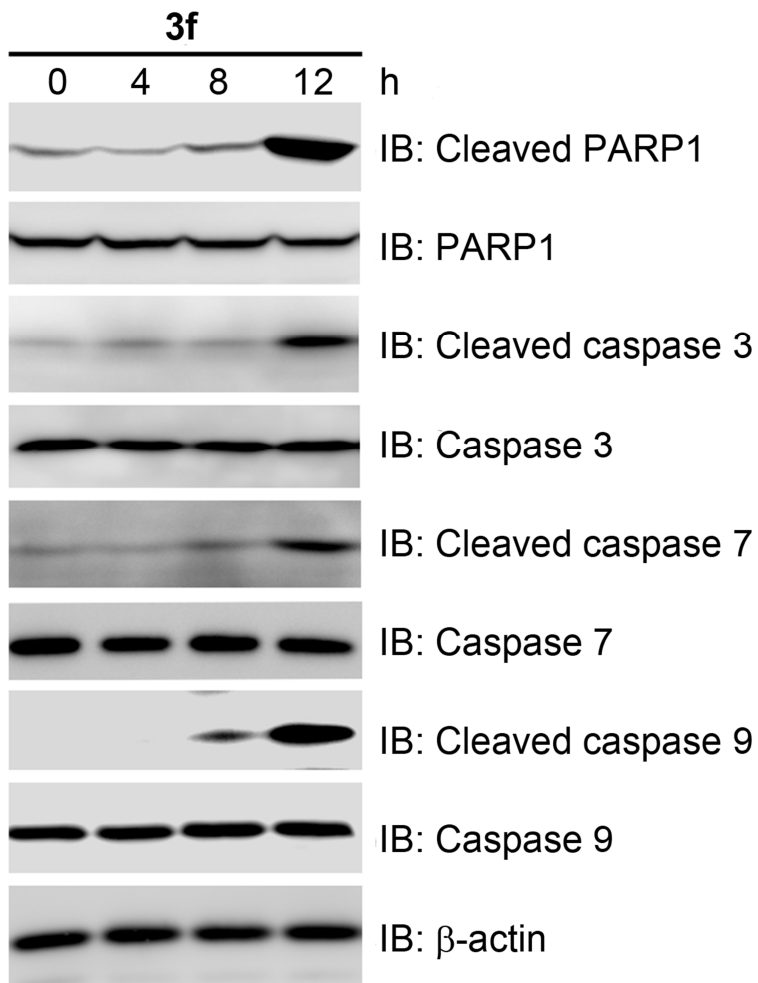
D

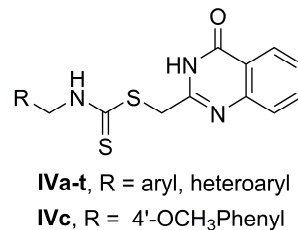
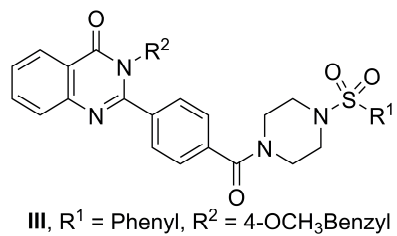
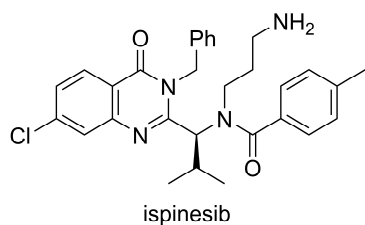
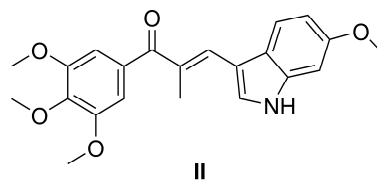
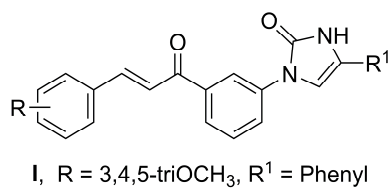
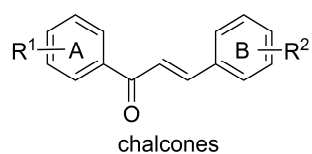


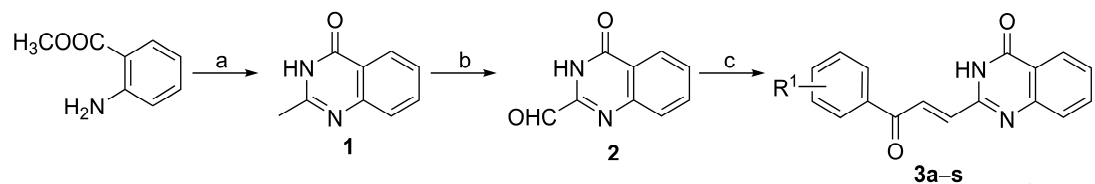


ACCEPTED MA

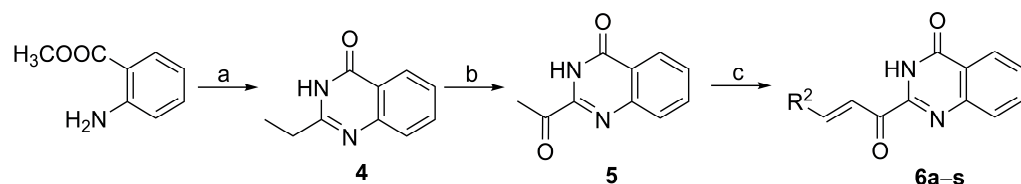








- a:** $R^1 = \text{H}$ **k:** $R^1 = 4\text{'-OH-3'-OCH}_3$
b: $R^1 = 2\text{'-OCH}_3$ **l:** $R^1 = 2\text{'-CH}_3$
c: $R^1 = 3\text{'-OCH}_3$ **m:** $R^1 = 4\text{'-CH}_3$
d: $R^1 = 4\text{'-OCH}_3$ **n:** $R^1 = 2',4\text{'-diCH}_3$
e: $R^1 = 2',4\text{'-diOCH}_3$ **o:** $R^1 = 4\text{'-Br}$
f: $R^1 = 2',5\text{'-diOCH}_3$ **p:** $R^1 = 4\text{'-Cl}$
g: $R^1 = 2',4',6\text{'-triOCH}_3$ **q:** $R^1 = 3',4\text{'-diCl}$
h: $R^1 = 3',4',5\text{'-triOCH}_3$ **r:** $R^1 = 4\text{'-F}$
i: $R^1 = 4\text{'-NH}_2$ **s:** $R^1 = 4\text{'-CF}_3$
j: $R^1 = 4\text{'-OH}$



- 6a-s**
- | | |
|---|--|
| a: $R^2 = C_6H_5$ | k: $R^2 = 4\text{-ClC}_6H_4$ |
| b: $R^2 = 2\text{-OCH}_3C_6H_4$ | l: $R^2 = 4\text{-FC}_6H_4$ |
| c: $R^2 = 3\text{-OCH}_3C_6H_4$ | m: $R^2 = 4\text{-CNC}_6H_4$ |
| d: $R^2 = 4\text{-OCH}_3C_6H_4$ | n: $R^2 = 4\text{-NO}_2C_6H_4$ |
| e: $R^2 = 2',4\text{-diOCH}_3C_6H_3$ | o: $R^2 = \text{Furan-2-yl}$ |
| f: $R^2 = 3',4\text{-diOCH}_3C_6H_3$ | p: $R^2 = \text{Thiophen-2-yl}$ |
| g: $R^2 = 3',5\text{-diOCH}_3C_6H_3$ | q: $R^2 = \text{Pyridin-2-yl}$ |
| h: $R^2 = 3',4',5\text{-triOCH}_3C_6H_2$ | r: $R^2 = \text{Pyridin-3-yl}$ |
| i: $R^2 = 4\text{-CH}_3C_6H_4$ | s: $R^2 = \text{Pyridin-4-yl}$ |
| j: $R^2 = 4\text{-BrC}_6H_4$ | |

ACCEPTED MANUSCRIPT

Research highlights

- Two series of chalcone analogues containing a 4-oxoquinazolin-2-yl group were synthesized.
- Compound **3f** is the most cytotoxic one with IC₅₀s of 3.56 and 4.08 μ M in HCT-116 and MCF-7 cells.
- HCT-116 cells treated with **3f** accumulated in the sub-G1 phase of the cell cycle.
- **3f**-induced apoptosis was confirmed by Annexin V, AO-EB, MitoSOXTM Red and JC-1 staining assays.
- **3f** increased the levels of cleaved PARP1, caspases 3, 7 and 9, activating the mitochondrial death pathway.